Caustic Analysis in Accelerators

Tessa Charles

University of Liverpool
Cockcroft Institute

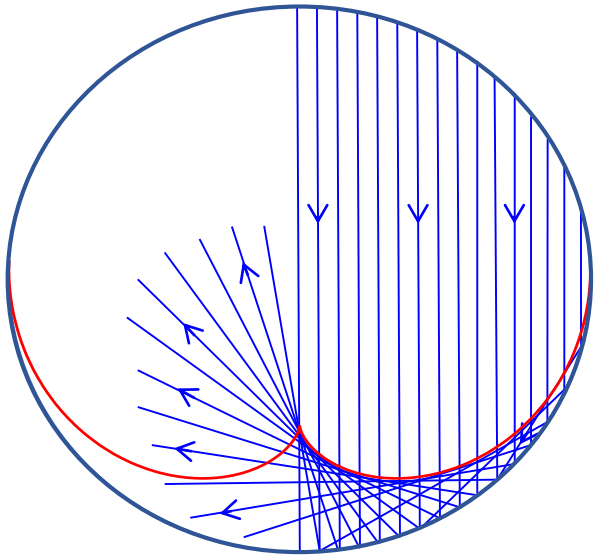

The envelope of trajectories forms the caustics lines.

Caustics lines are an envelope of trajectories, or the projection of that envelope on another surface.

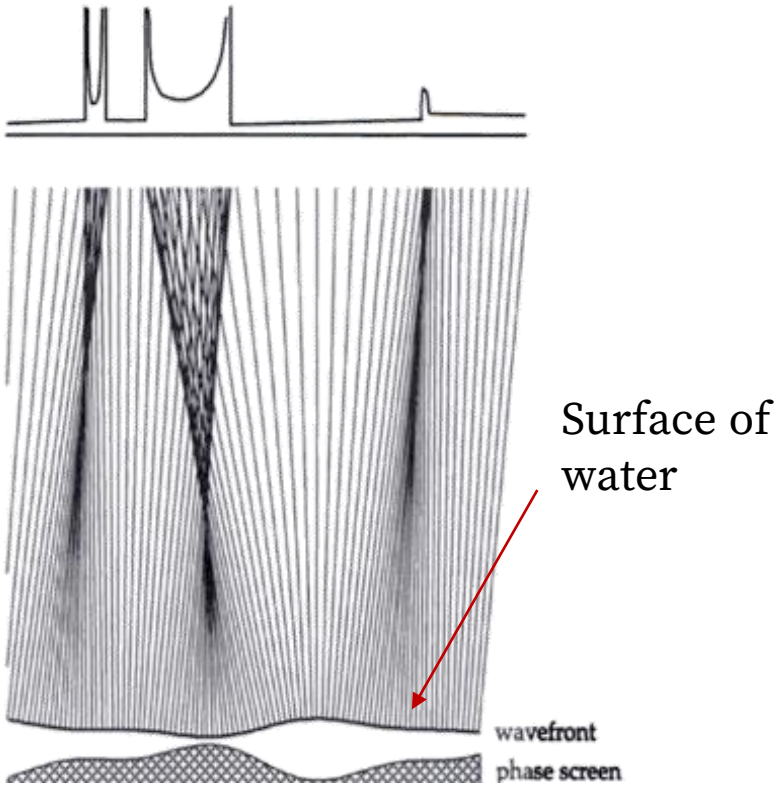

J.F. Nye Natural Focusing and Fine Structure of Light: Caustics and Wave Dislocations", (Taylor & Francis, Philadelphia, 1999).

Caustics lines are an envelope of trajectories,
or the projection of that envelope on another surface.

Outline

1. Introduction of caustics
2. Current horn suppression
3. MAX IV experimental measurements
4. Longitudinal Phase Space manipulation in recirculating machines
5. Microbunching instability

Outline

1. Introduction of caustics
2. Current horn suppression *(example of the usefulness of caustics)*
3. MAX IV experimental measurements
4. Longitudinal Phase Space manipulation in recirculating machines *(example of the usefulness of caustics)*
5. Microbunching instability *(example of the usefulness of caustics)*

Electron trajectories in a bunch compressor:

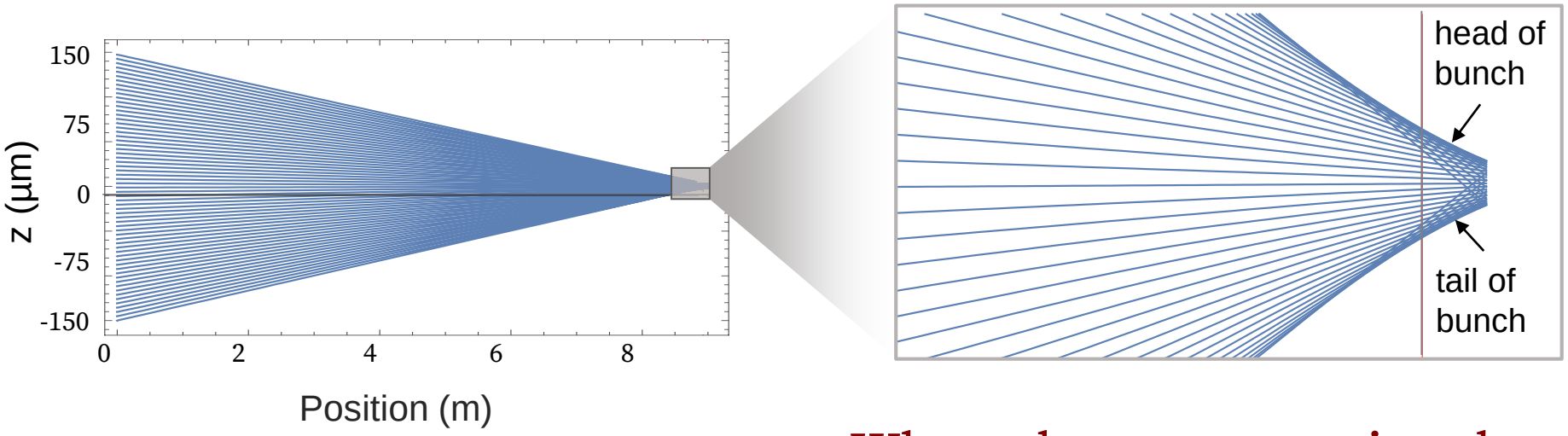

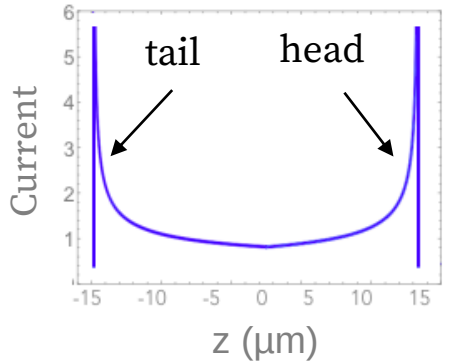

Where there are caustics, there will be current spikes.

Optical caustics example:

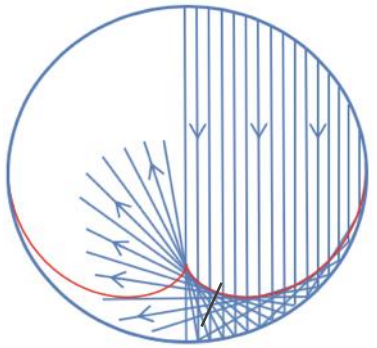

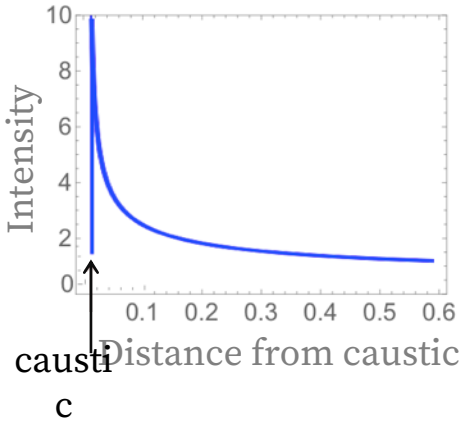

Caustics are singularities in the density of families of trajectories.

Caustics fall into catastrophe theory

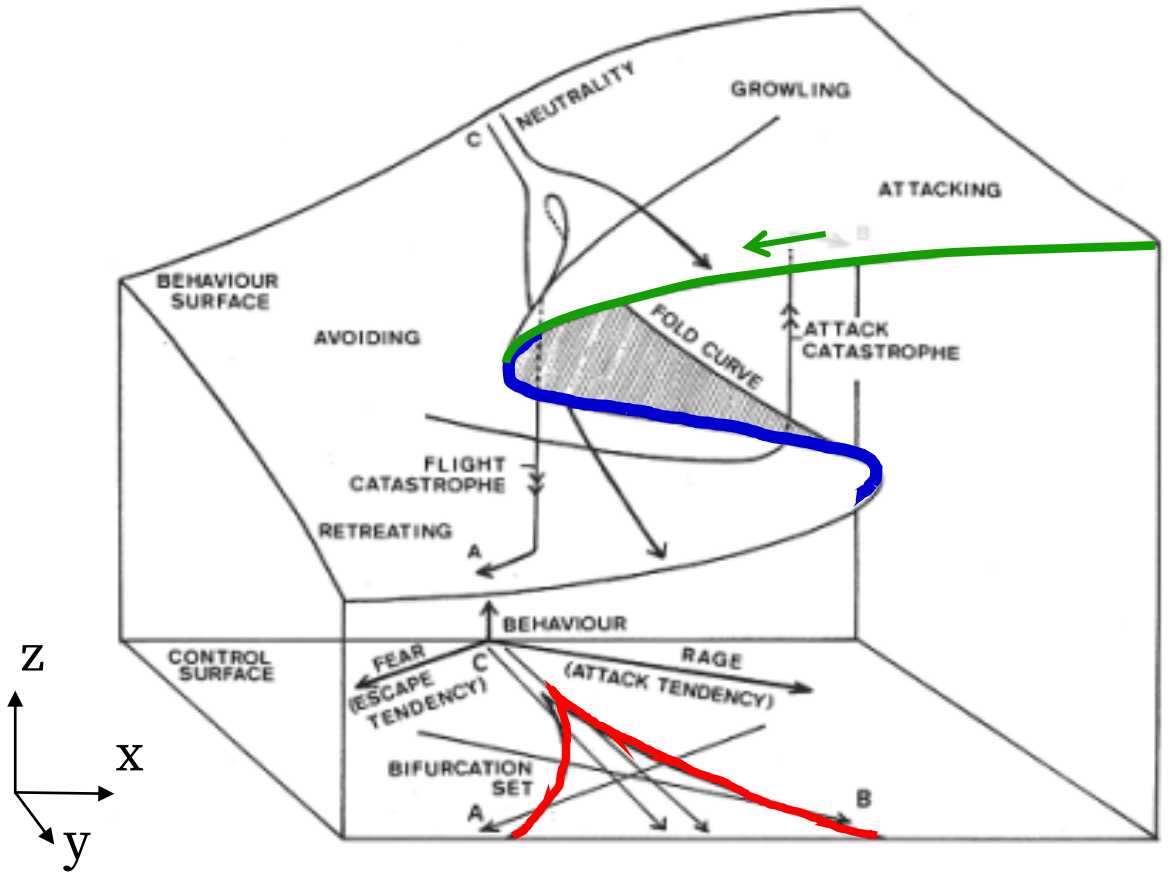

Figure: EC Zeeman (1976) Catastrophe Theory in Scientific American.

Longitudinal phase space evolution through a bunch compression

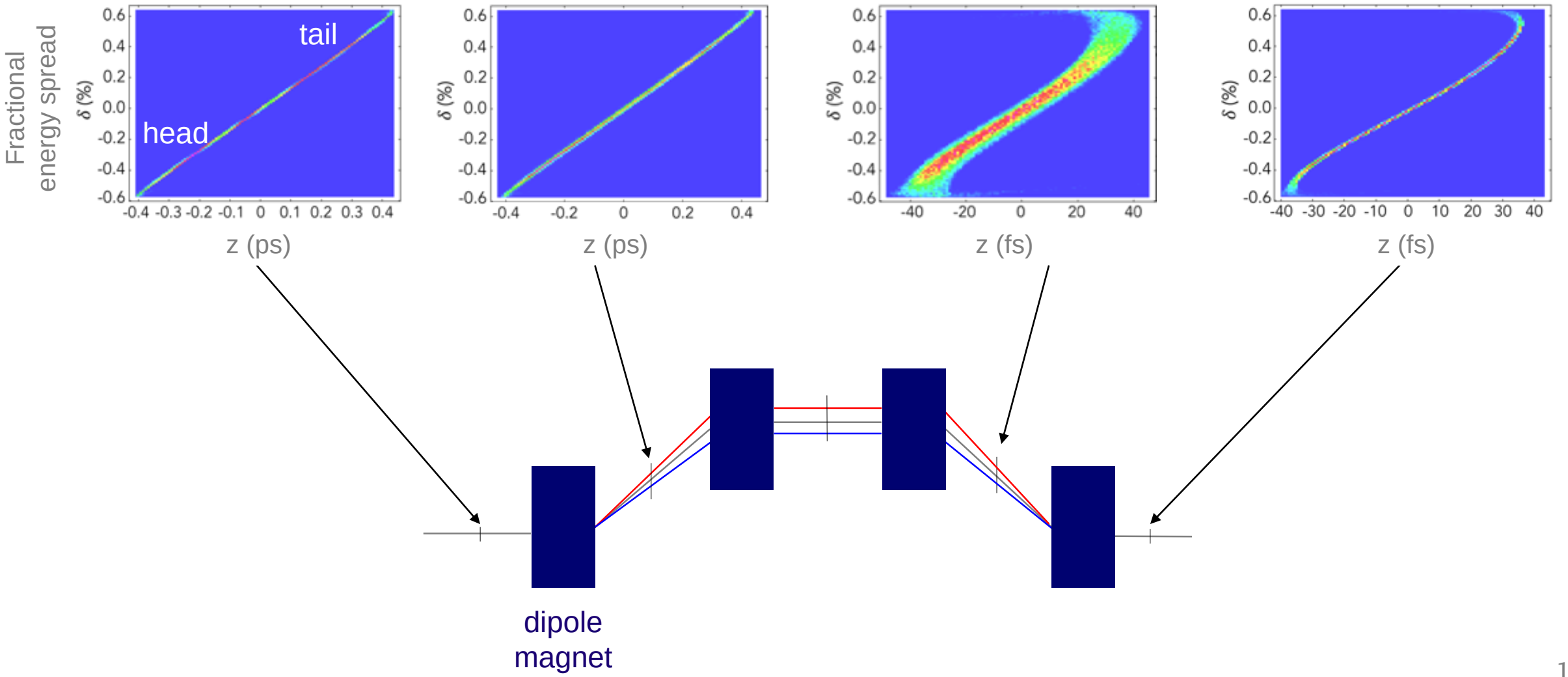

Longitudinal phase space dist. at bunch compression exit

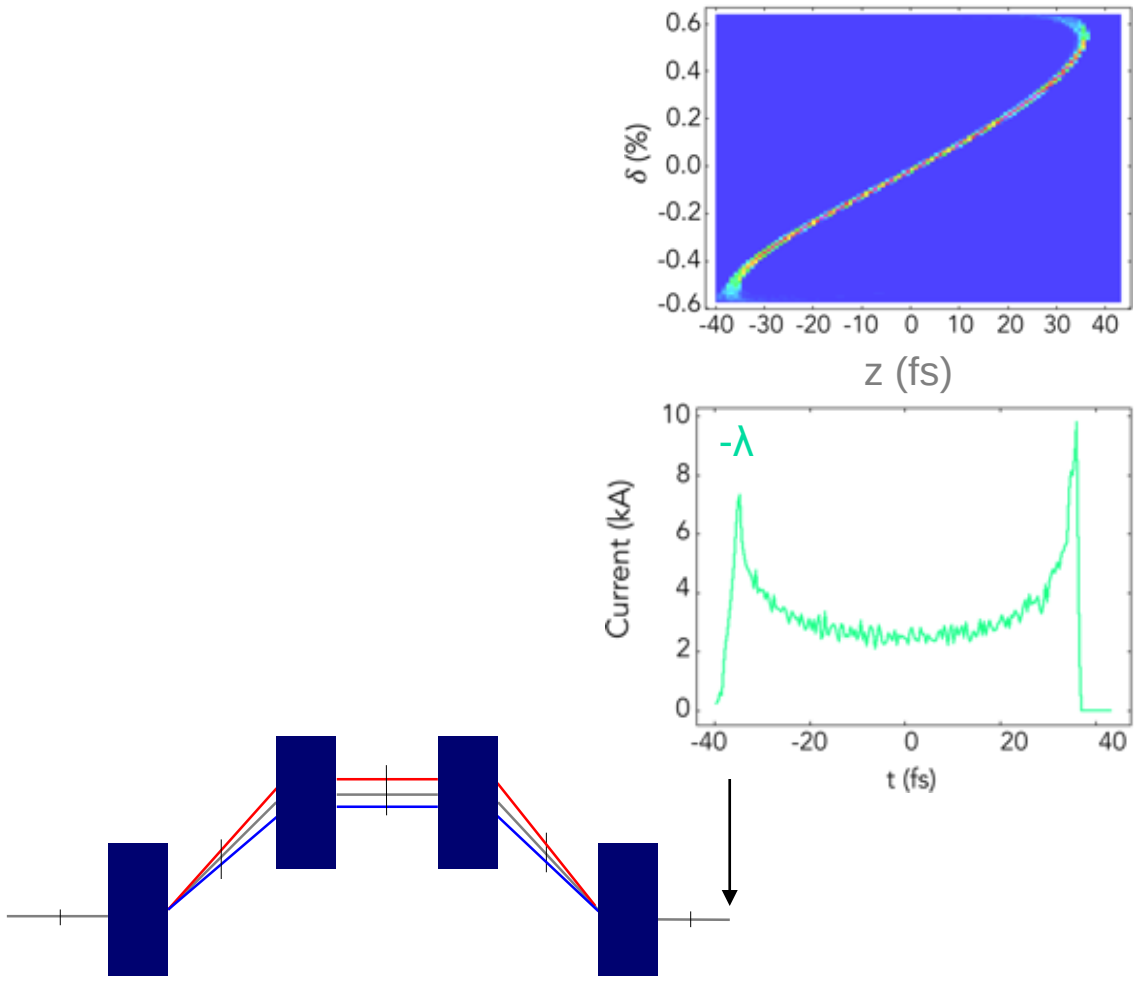

Energy spread induced by Coherent Synchrotron Radiation (CSR):

λ = linear charge density

$$\frac{dE}{cdt} = \frac{-2e^2}{4\pi\epsilon_0(3R^2)^{1/3}} \int_{\tilde{z}-z_L}^{\tilde{z}} \frac{d\lambda}{dz} \left(\frac{1}{\tilde{z}-z}\right)^{1/3} dz$$

Current spikes are problematic, leading to **CSR-induced emittance growth.**

Caustic expression:

$$\tilde{z}_c(z_i) = z_i + \frac{\delta(z_i)(-1 + T_{566}(-2 + \delta(z_i))\delta'(z_i) + U_{5666}(-3 + \delta(z_i)^2)\delta'(z_i))}{\delta'(z_i)}$$

$$\tilde{R}_{56}(z_i) = \frac{-1 - 2T_{566}\delta'(z_i) - 3U_{5666}\delta'(z_i)}{\delta'(z_i)}$$

Initial phase space distribution:

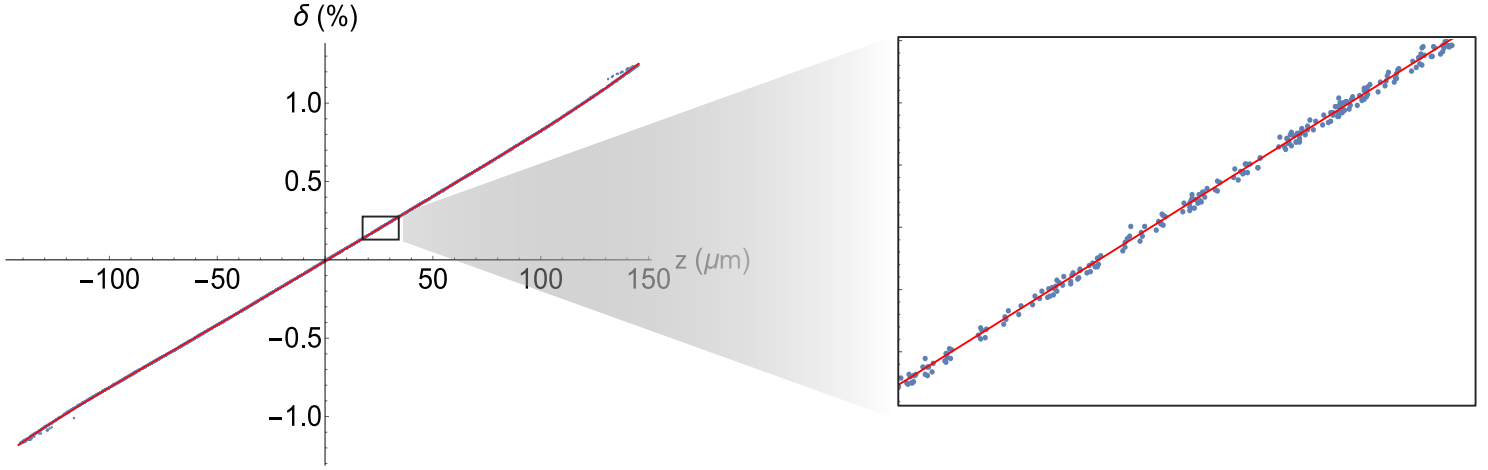

$$\delta(z_i) = h_1 z_i + h_2 z_i^2 + h_3 z_i^3$$

T.K.Charles et al. Phys. Rev. Accel. Beams, (2016) **19**, 104402

Caustic expression for a chicane

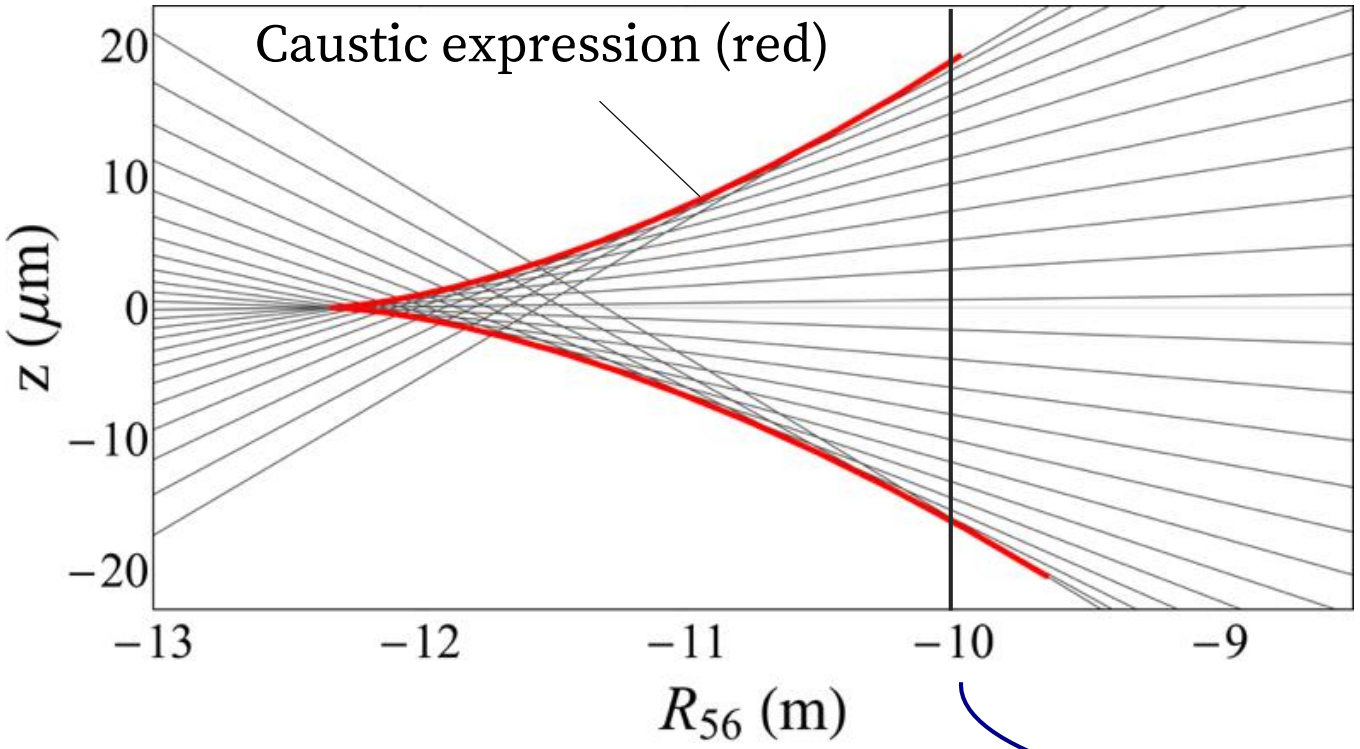

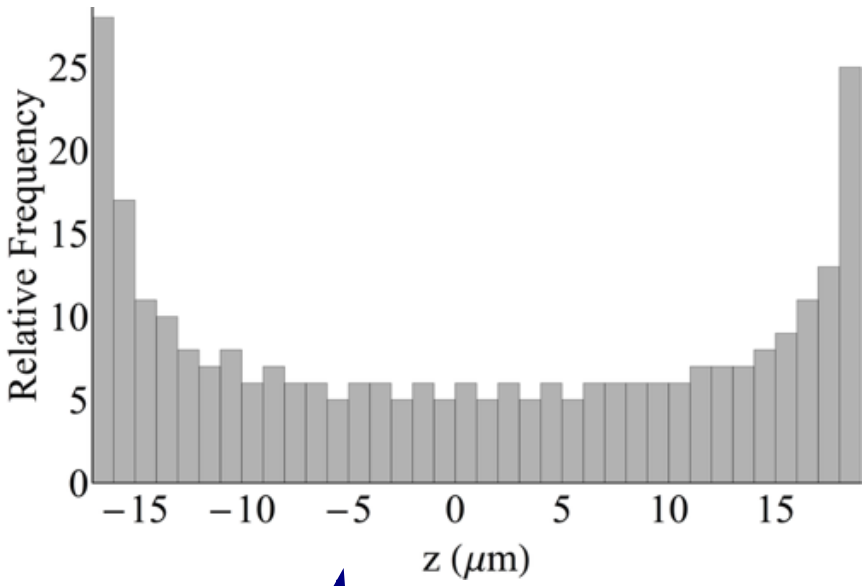

R_{56} = -10 mm

Fold

T_{566} = 18.1 mm, U_{5666} = -24 mm

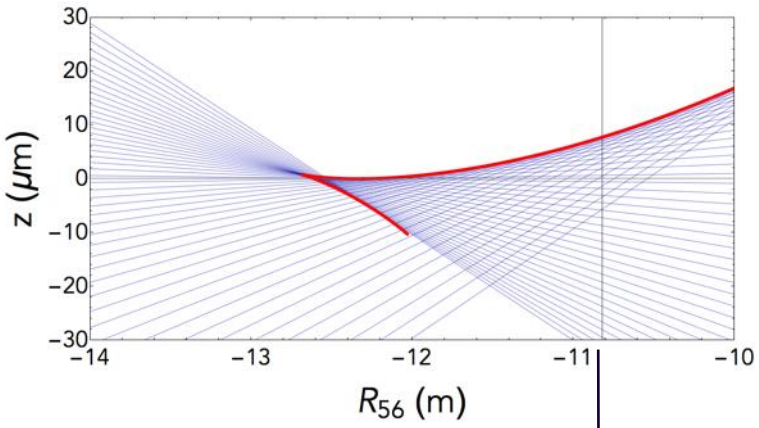

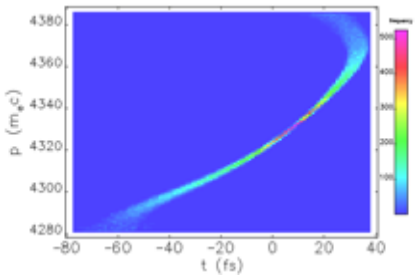

E.g. single spike bunch compression [S. Huang *et al,* Phys. Rev. AB (2014) 17 120703]

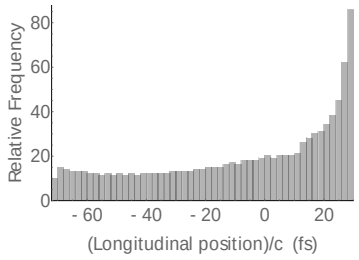

Cusp

T_{566} = 16.4 mm, U_{5666} = -11.4 mm

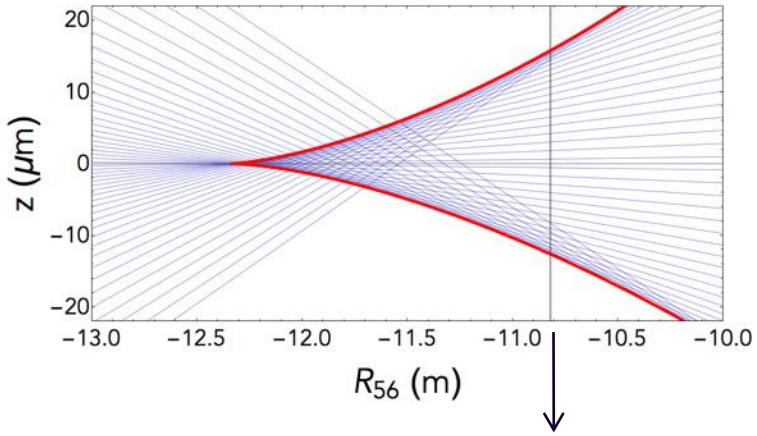

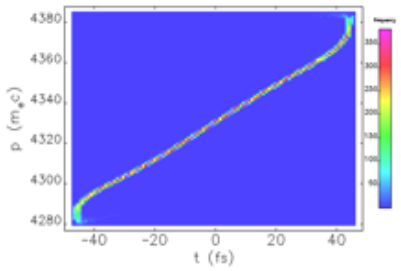

E.g. LCLS [Y. Ding *et al.* Phys. Rev. AB 19, 100703]

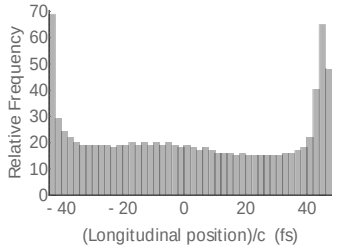

Butterfly

T_{566} =16.1 mm, U_{5666} = 2.6 m

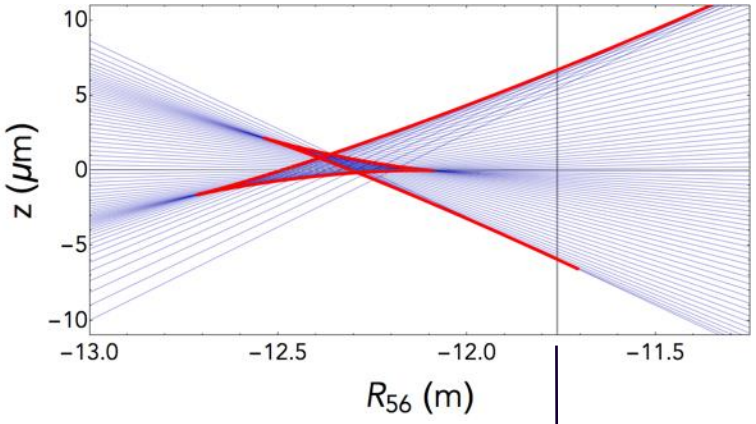

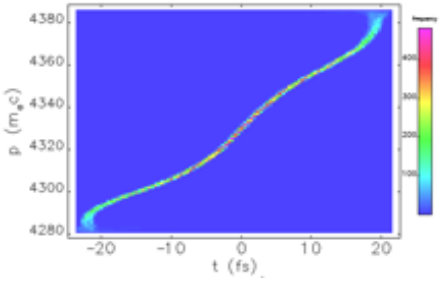

E.g. MAX IV [S. Thorin *et al*. FEL2010, WEPB34]

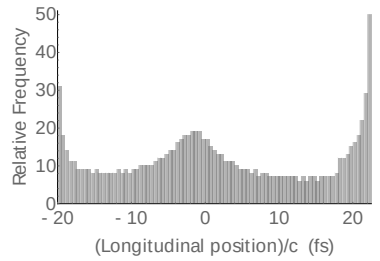

A closer look…

3 types of catastrophes, but all described by the same parametric expression.

$$\tilde{z}(z_i) = z_i + \frac{\delta(z_i)(-1 + T_{566}(-2 + \delta(z_i))\delta'(z_i) + U_{5666}(-3 + \delta(z_i)^2)\delta'(z_i))}{\delta'(z_i)}$$

$$\tilde{R_{56}}(z_i) = \frac{-1 - 2T_{566}\delta'(z_i) - 3U_{5666}\delta'(z_i)}{\delta'(z_i)}$$

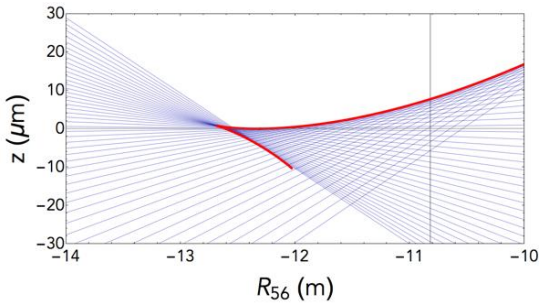

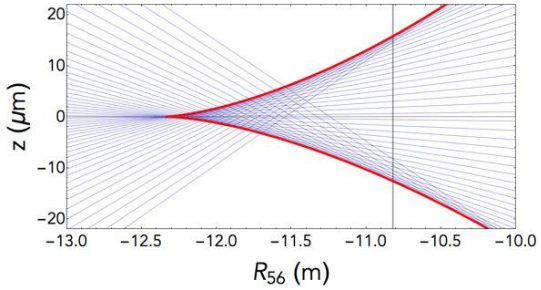

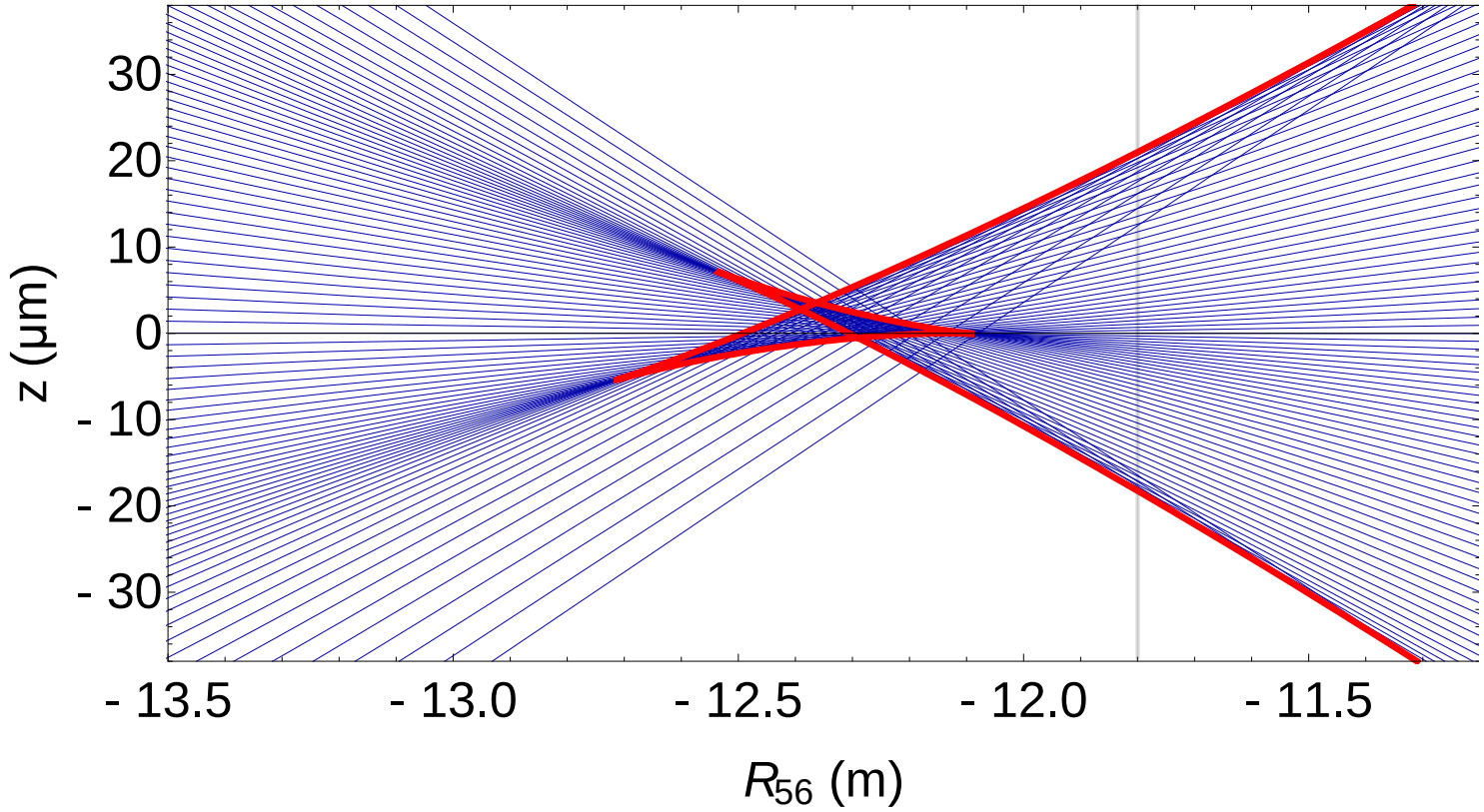

These 3 cases give us an idea of how we might be able to sculpt electron trajectories to our benefit.

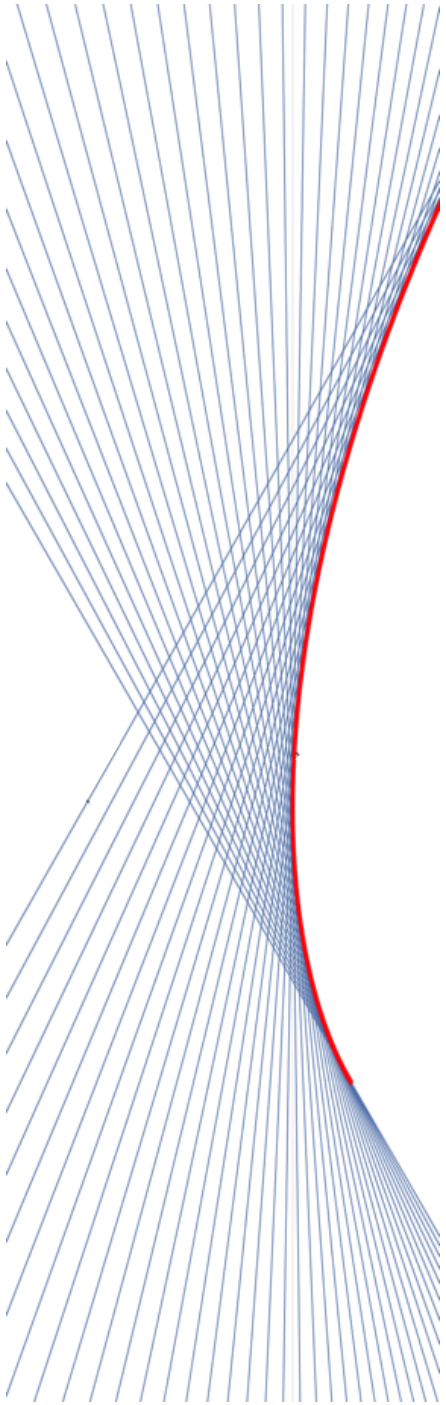

Current horn suppression

Example of the usefulness of caustics

LSLC's experience - current spikes diminish FEL performance

Before collimation

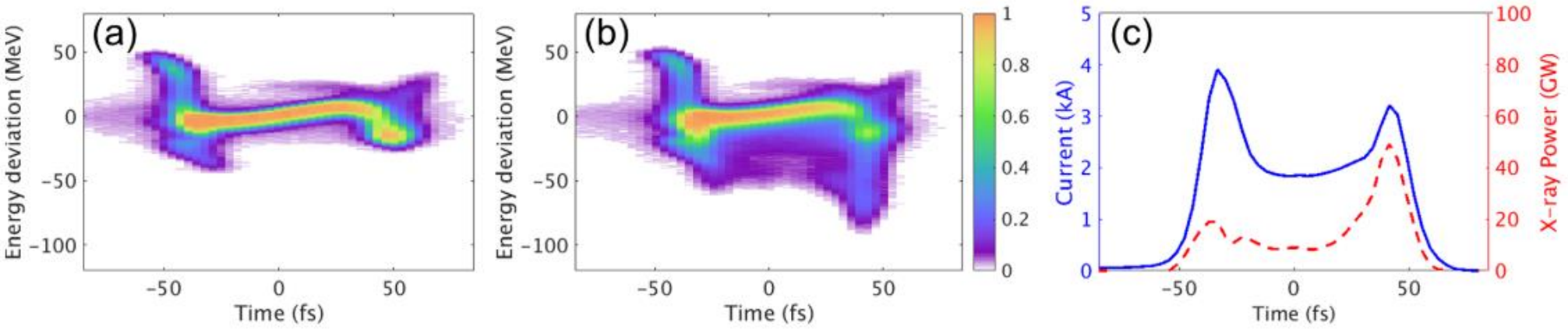

After collimation

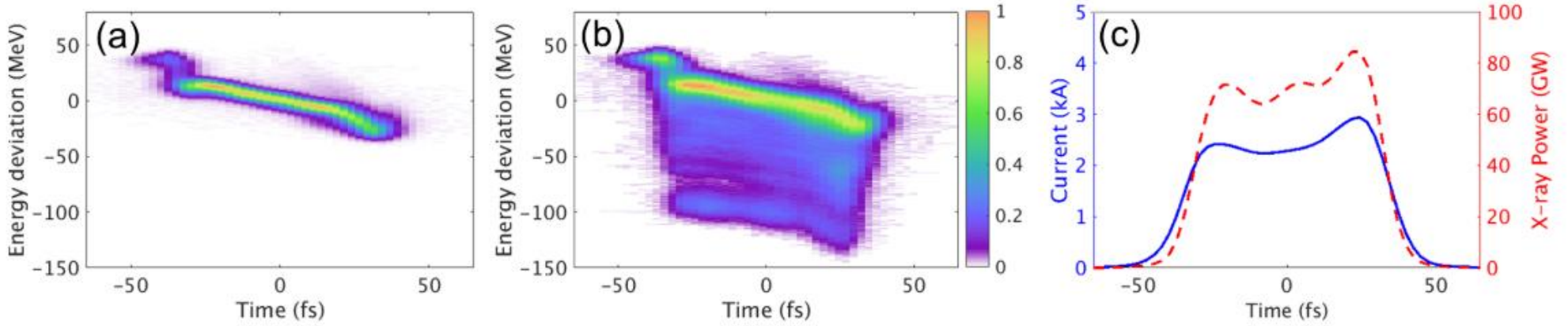

FEL power increased from ~3.5 mJ to 4-5 mJ.

Y. Ding et al. (2016) Phys. Rev. AB 19, 100703

Current horn suppression - an S-band FEL Linac example

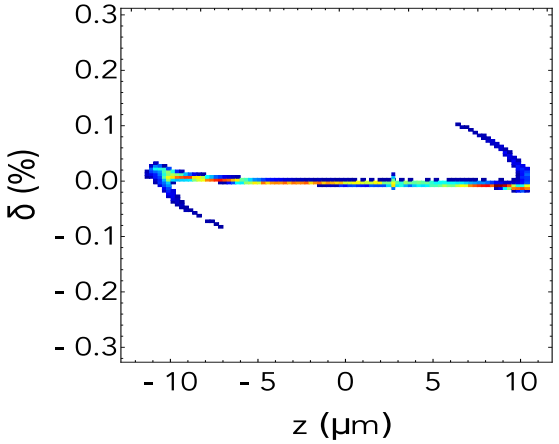

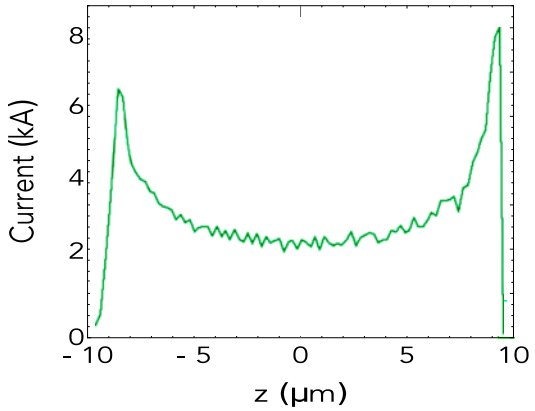

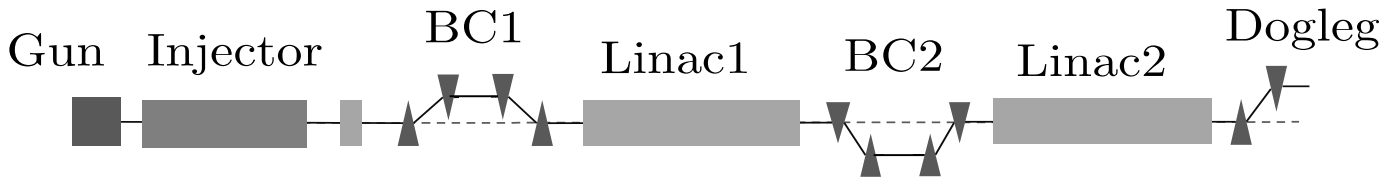

Elegant simulations of longitudinal phase space and current profile at the end of Linac2.

Caustic condition

$$R_{56}s\frac{d(\delta(z))}{dz}\bigg|_{z=z_i} + T_{566}s\frac{d}{dz}\left(\delta^2(z)\right)\bigg|_{z=z_i} + U_{5666}s\frac{d}{dz}\left(\delta^3(z)\right)\bigg|_{z=z_i} + s_{BC} = 0.$$

where,

δ = energy spread
z_i = initial longitudinal position
s = position along accelerator
s_{BC} = end of bunch compressor position

Point (a) is the working point of the S-band linac example

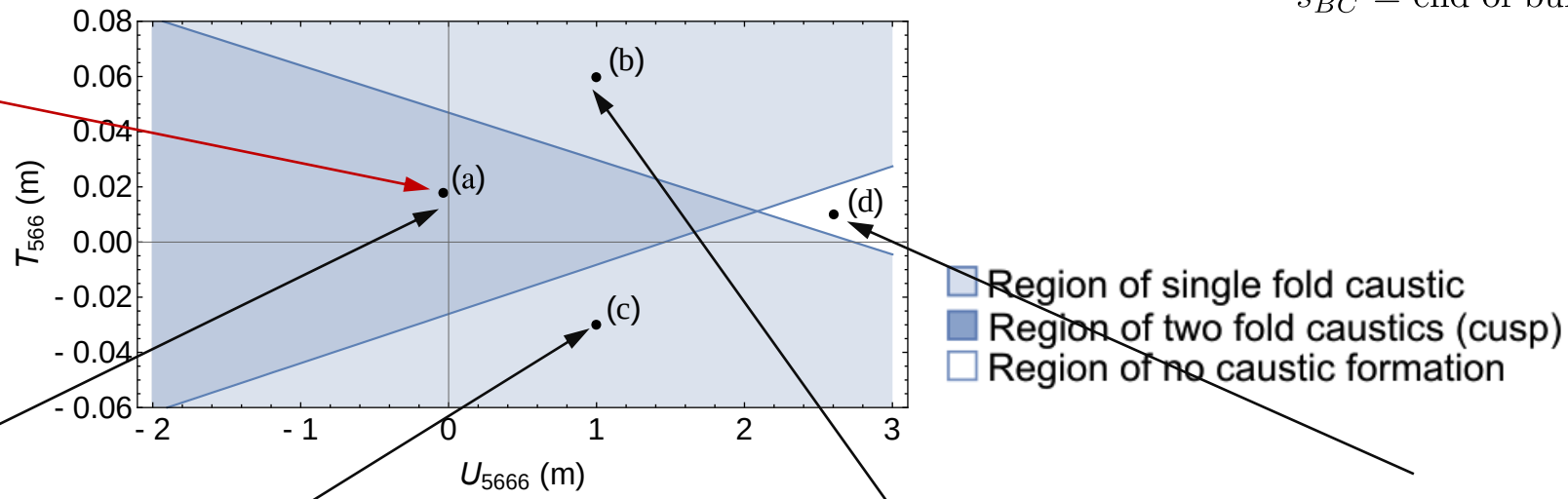

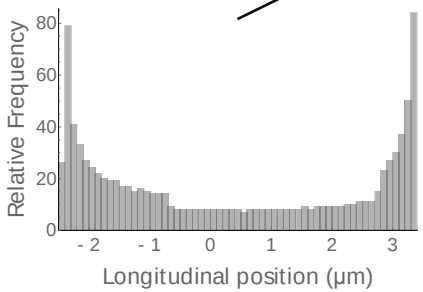

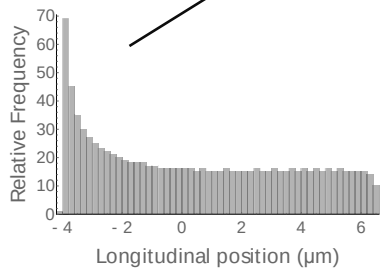

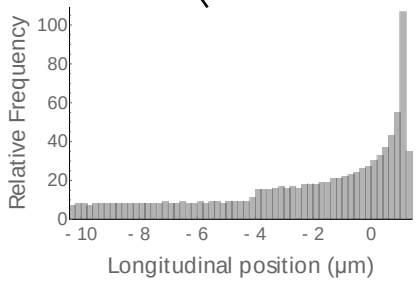

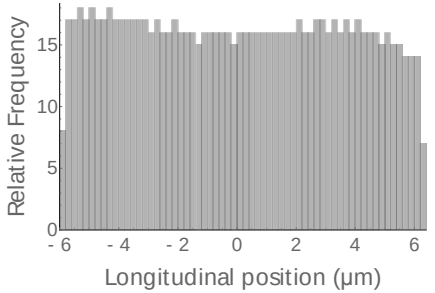

Caustic condition

$$R_{56}s\frac{d(\delta(z))}{dz}\bigg|_{z=z_i} + T_{566}s\frac{d}{dz}\left(\delta^2(z)\right)\bigg|_{z=z_i} + U_{5666}s\frac{d}{dz}\left(\delta^3(z)\right)\bigg|_{z=z_i} + s_{BC} = 0.$$

where,

δ = energy spread
z_i = initial longitudinal position
s = position along accelerator
s_{BC} = end of bunch compressor position

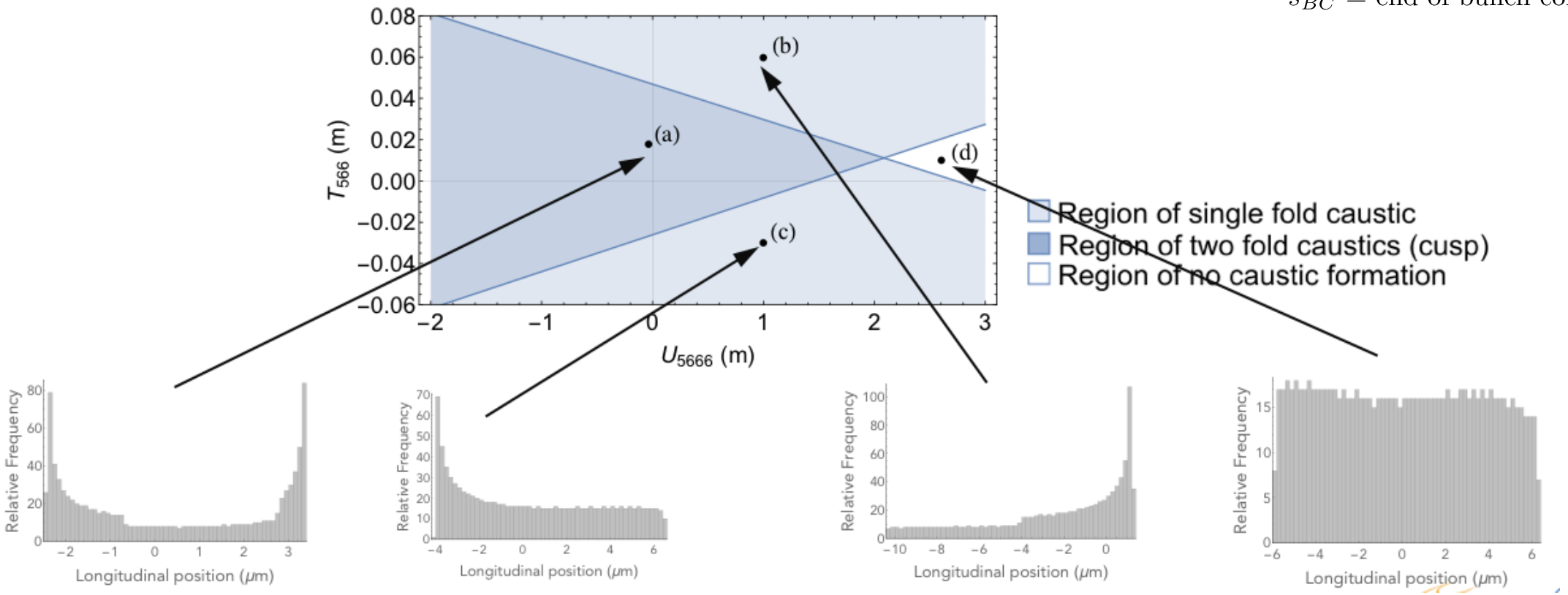

Caustic current horn suppression - S-band FEL linac

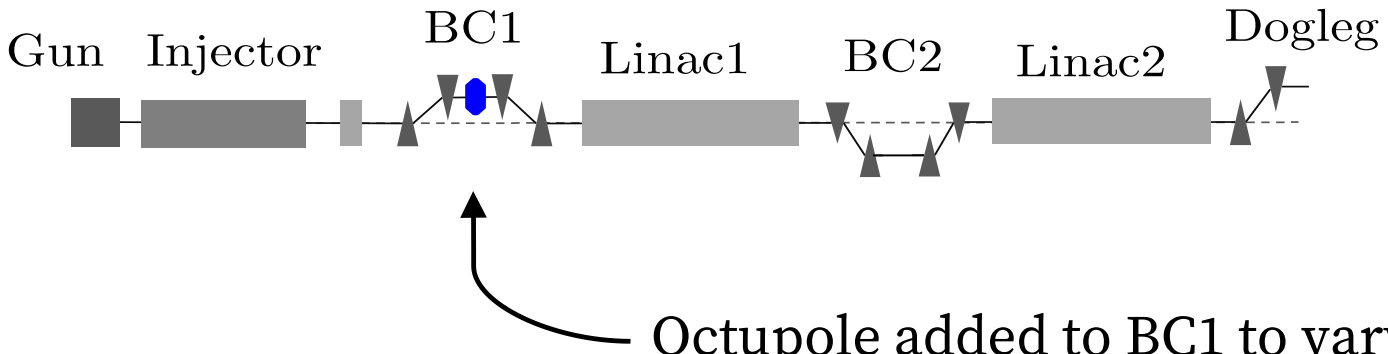

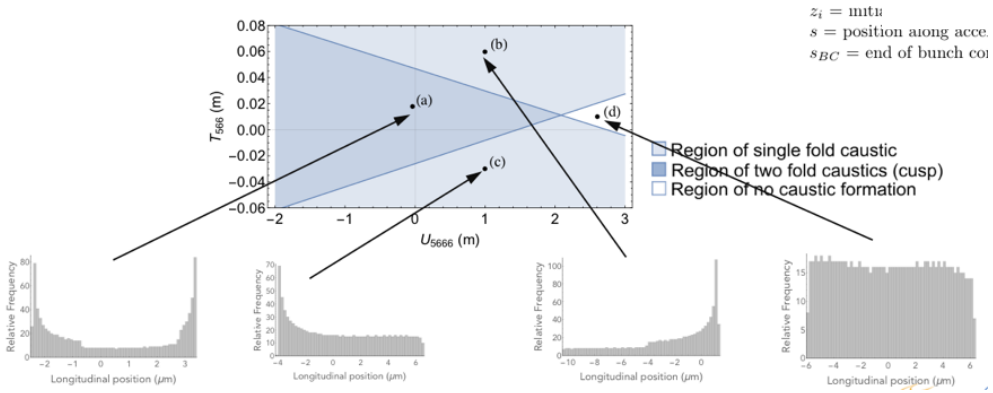

Caustic current horn suppression - S-band FEL linac

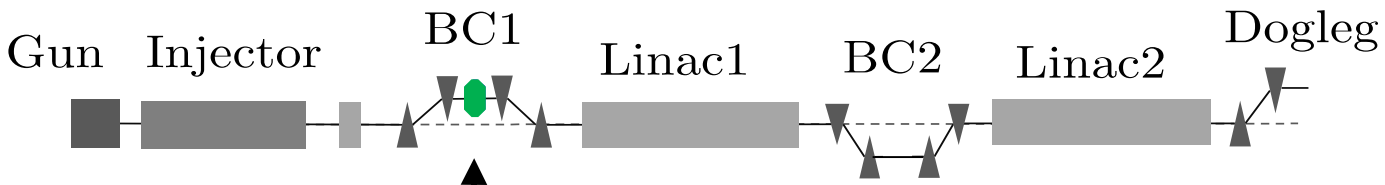

Octupole added to BC1 to vary U5666.

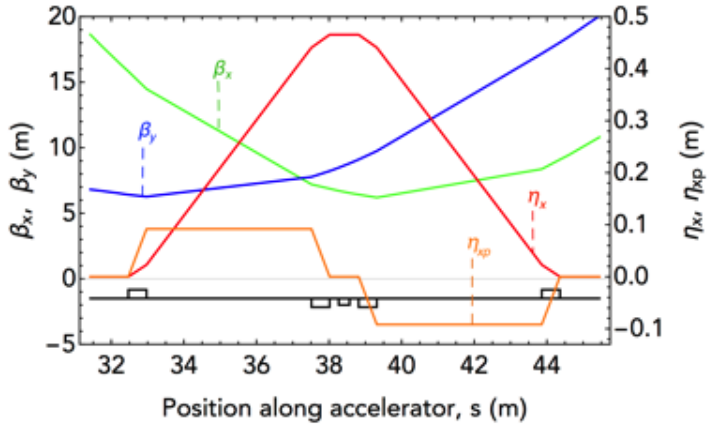

BC1:
R56 = -82.36 mm
T566 = 102.40 mm
U5666 = -5.23 m

Dipole bending angle, $\theta = 5.25°$
Octupole strength, K3 =2061 m^{-4}

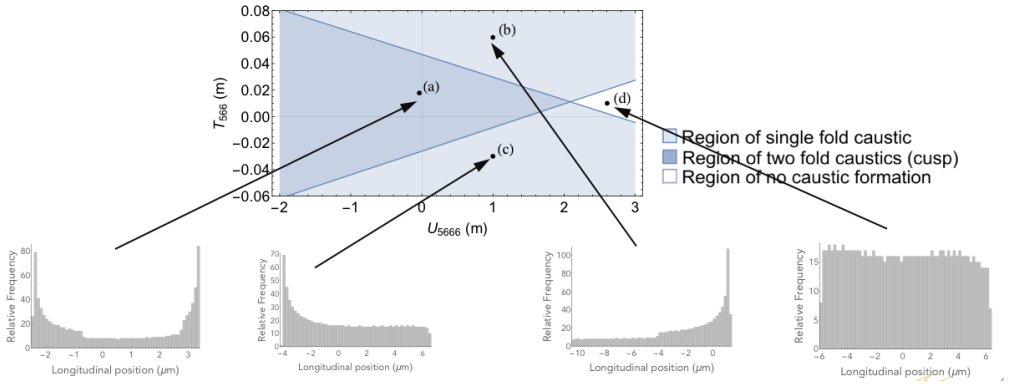

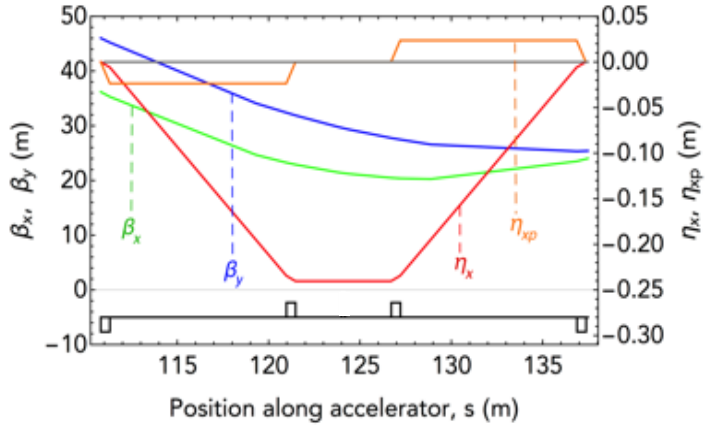

BC2:
R56 = -11.18 mm
T566 = 32.10 mm
U5666 = -72.19 mm

Dipole bending angle, $\theta = 1.35°$
Sextupole 1 strength, K2 = 11.03 m^{-3}

Caustic current horn suppression

***Without* octupole:**

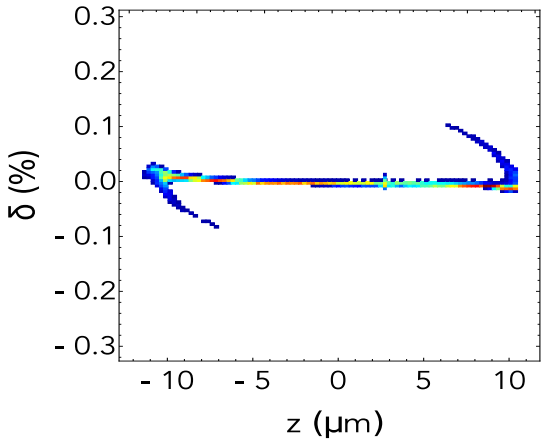

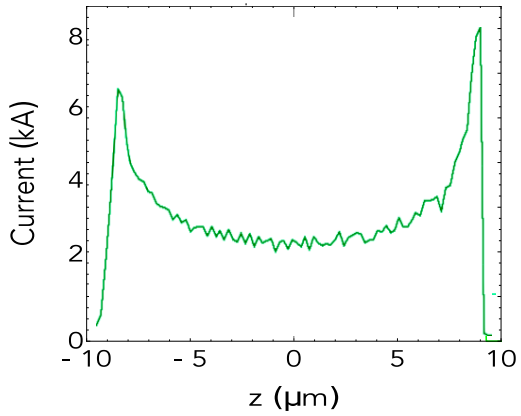

$\epsilon_{nx} = 1.359$ mm mrad

***With* octupole:**

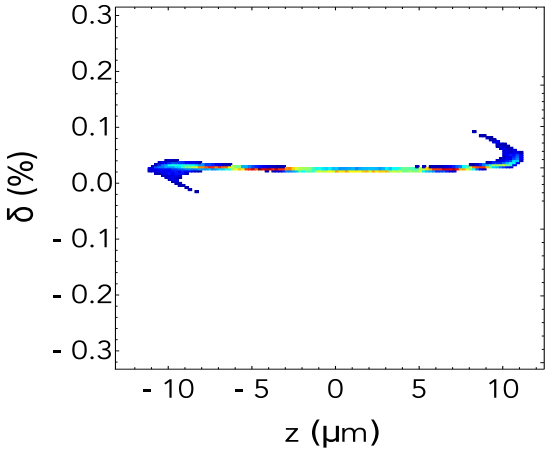

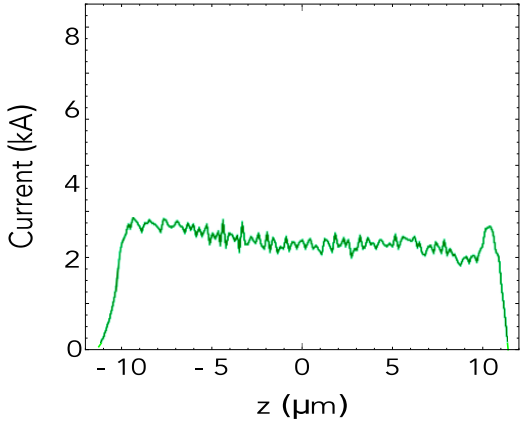

$\epsilon_{nx} = 0.762$ mm mrad

63% reduction in the CSR-induced emittance growth.

T.K.Charles et al. Phys. Rev. Accel. Beams, (2017) **20**, 030705

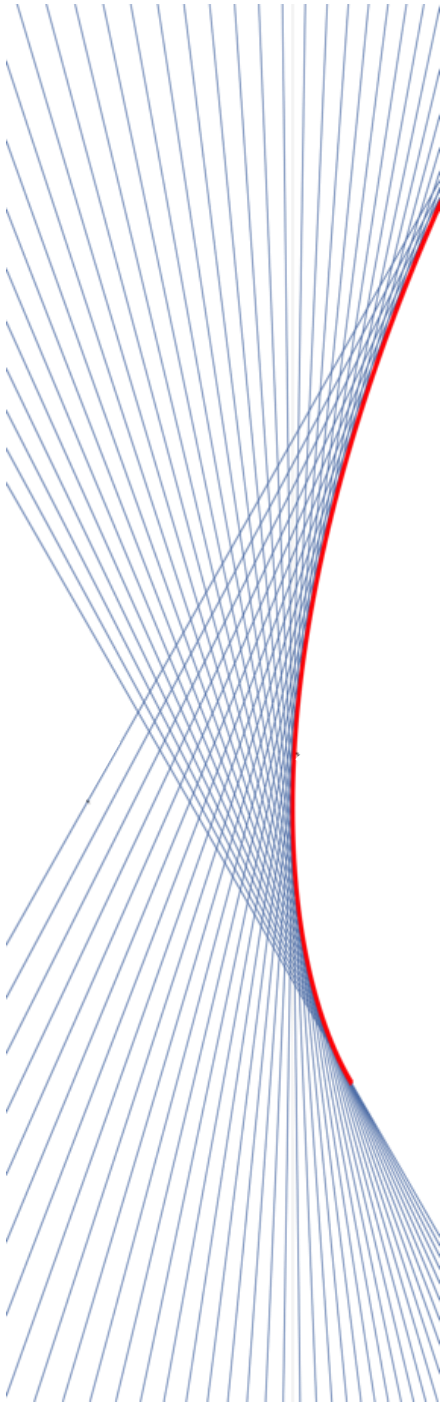

Experimental results from MAX IV

with Andrea Latina (CERN), Sara Thorin (MAX IV), Jonas Björklund Svensson (MAX IV)

MAX IV

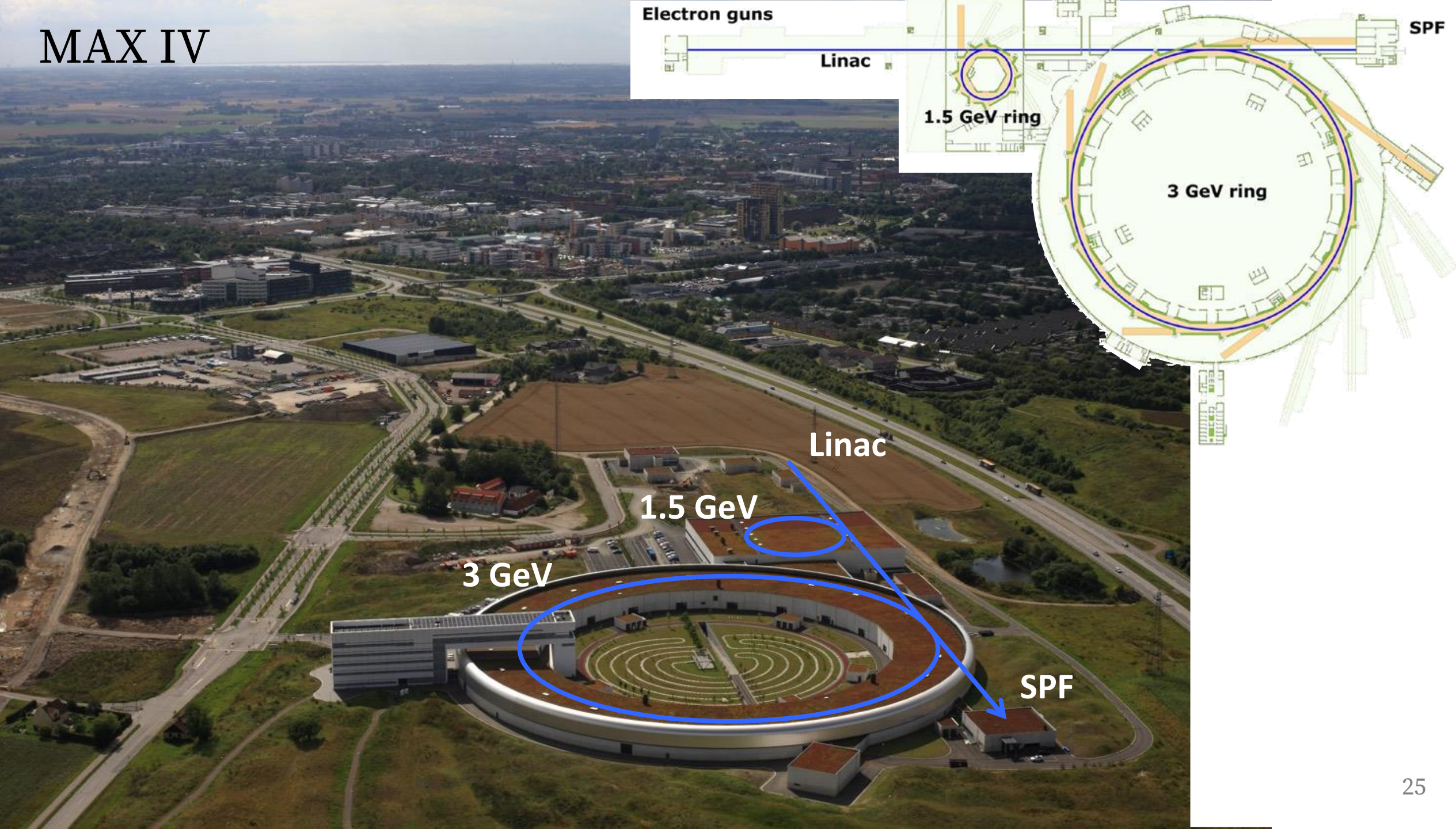
Electron guns
Linac
1.5 GeV ring
SPF
3 GeV ring
Linac
1.5 GeV
3 GeV
SPF

MAX IV Linac

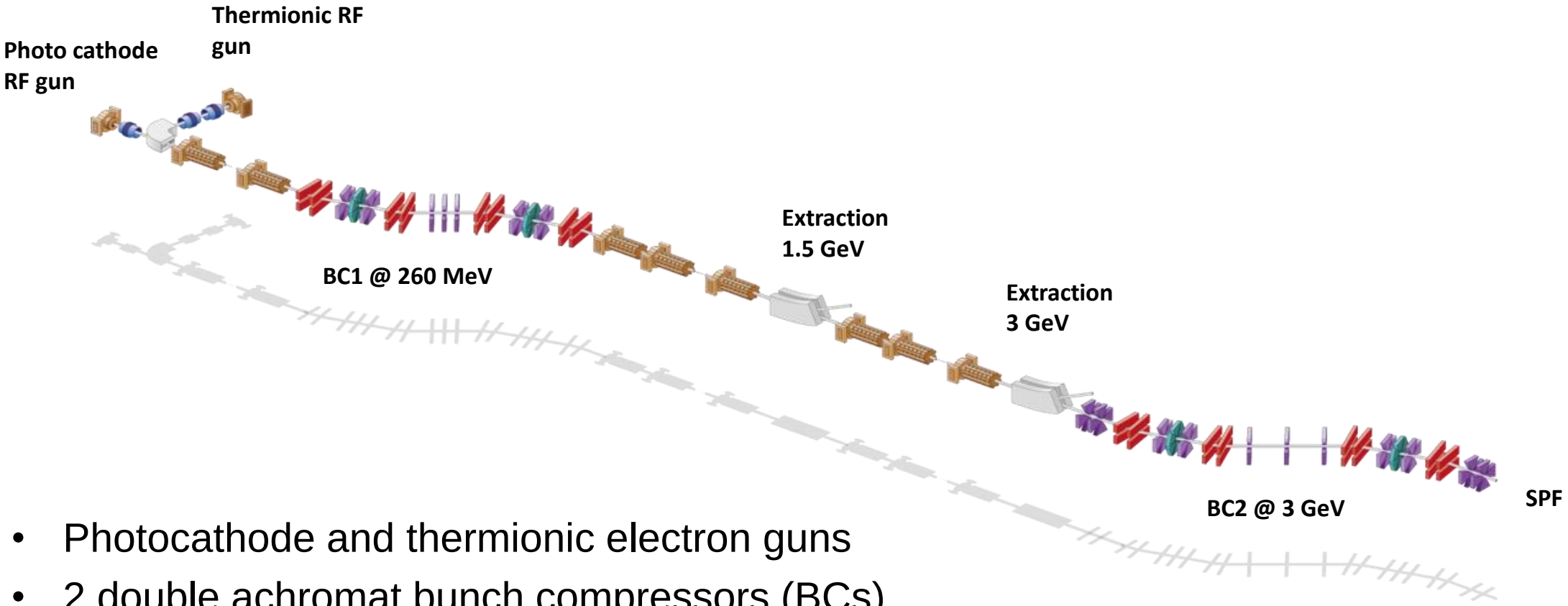

- Photocathode and thermionic electron guns
- 2 double achromat bunch compressors (BCs)
- RF frequency 2.998 GHz

MAX IV Bunch Compressors

Double achromat bunch compressors:

- **positive fixed R56 (energy chirp from falling falling RF slope)**
- **natural T566 used for linearization, self-linearizing**
- **weak sextupoles at the center of each achromat used for fine tuning T566**

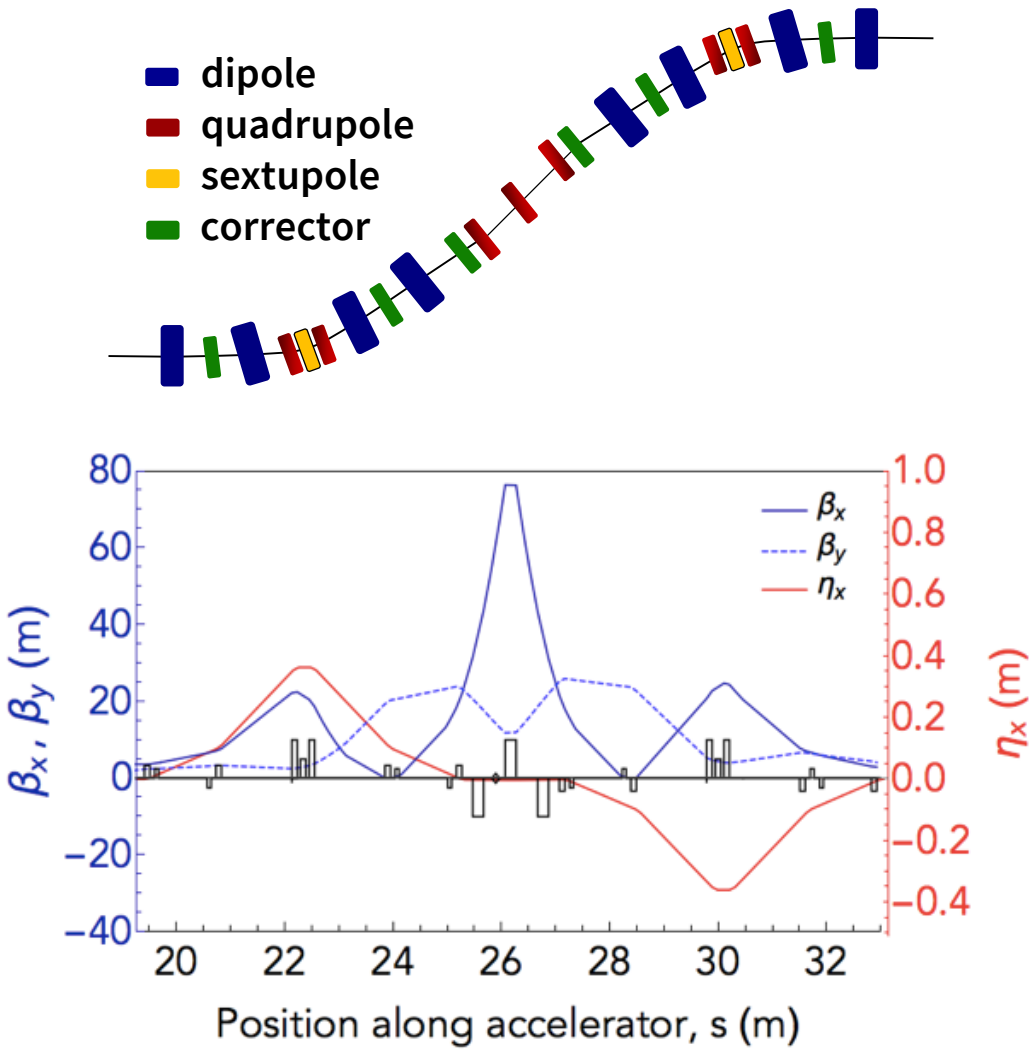

Zero-crossing method

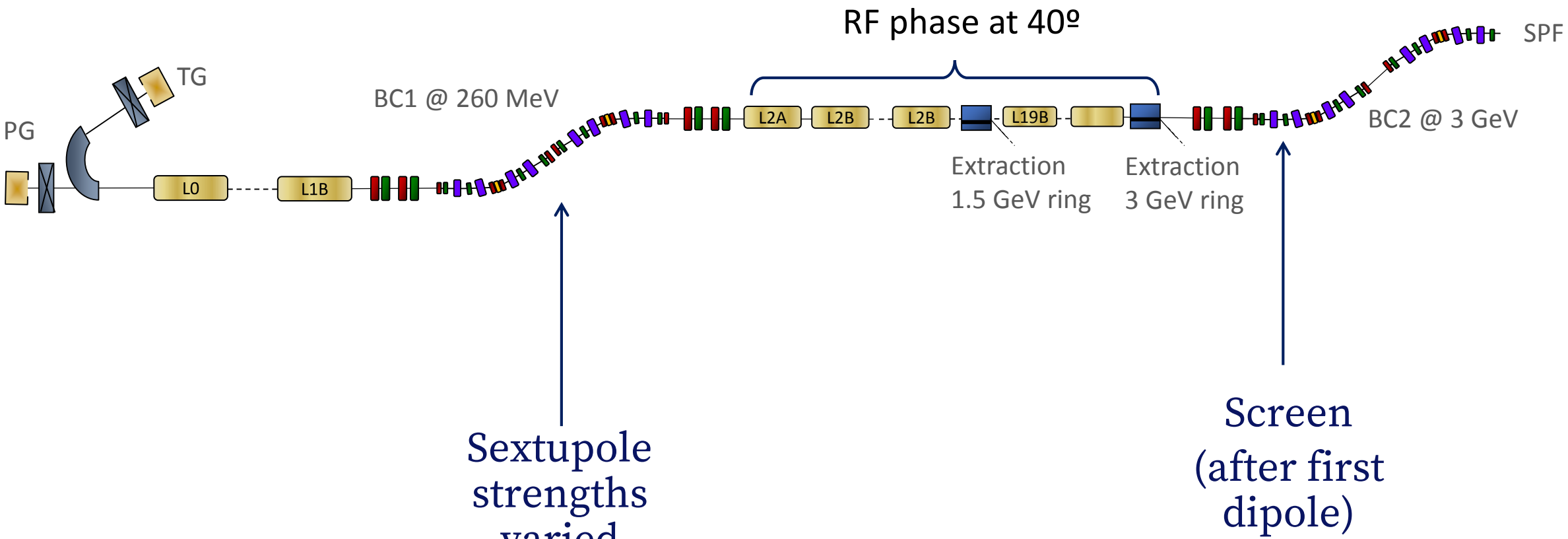

Zero-crossing method

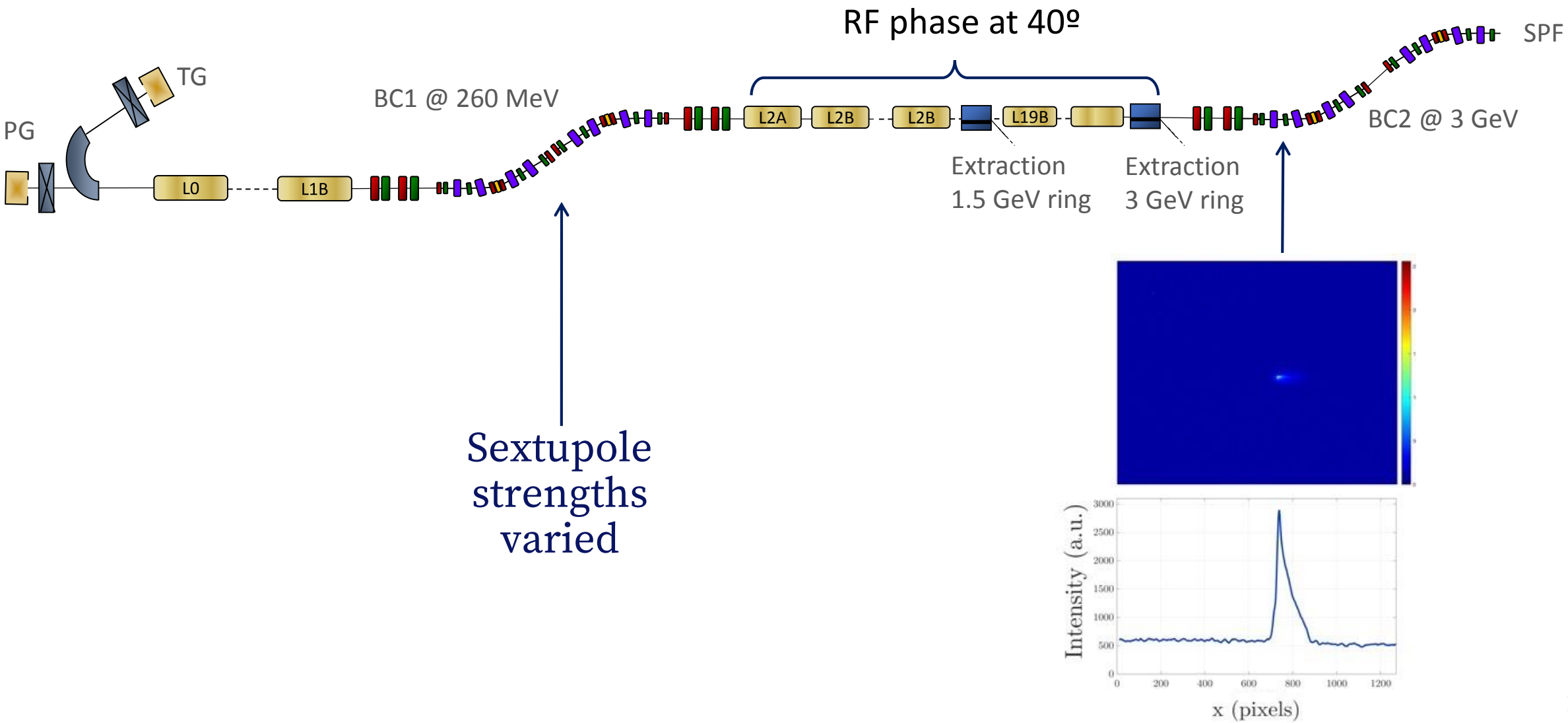

Experimental results – linearly ramped current profiles

Sextupole strengths [m^{-3}]:

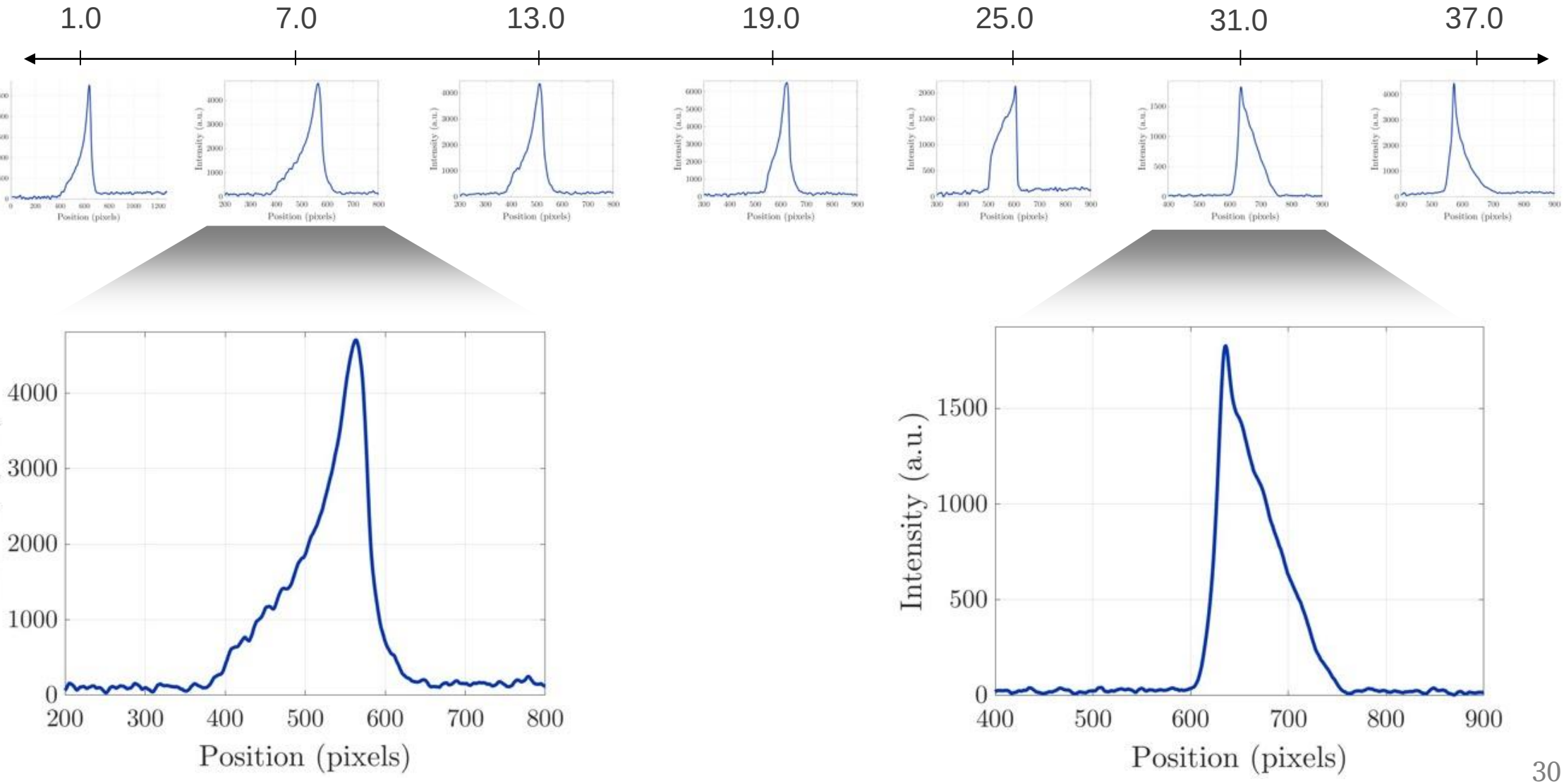

Illustration of compressed bunches

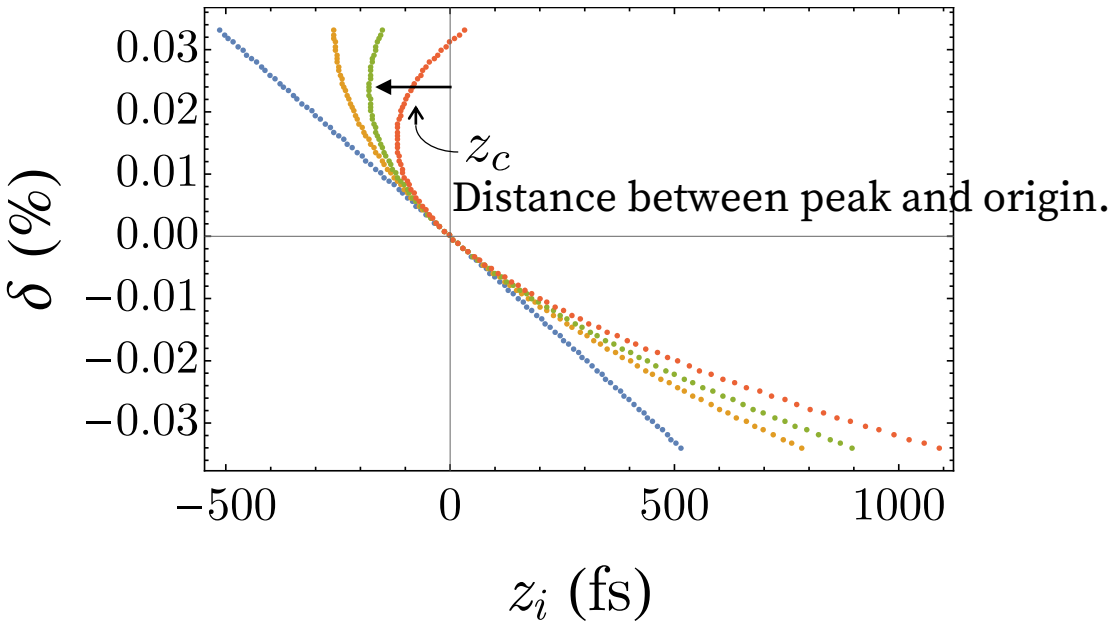

The origin is found as being the distance from one bunch edge to the position within the bunch where the accumulated integrated charge equals half of the total charge.

Caustic expression:

$$z_c(z_i) = -z_i - \frac{R_{56}\delta(z_i)}{2} + \frac{U_{5666}\ \delta^3(z_i)}{2} + \frac{\delta(z_i)}{2\delta'(z_i)}$$

$$\tilde{T}_{566}(z_i) = \frac{1}{2\delta(z_i)}\left(-R_{56} - \frac{1}{\delta'(z_i)} - 3U_{5666}\ \delta^2(z_i)\right)$$

(Same expression as shown on slide 11, simply re-arranged)

Mapping out caustic lines

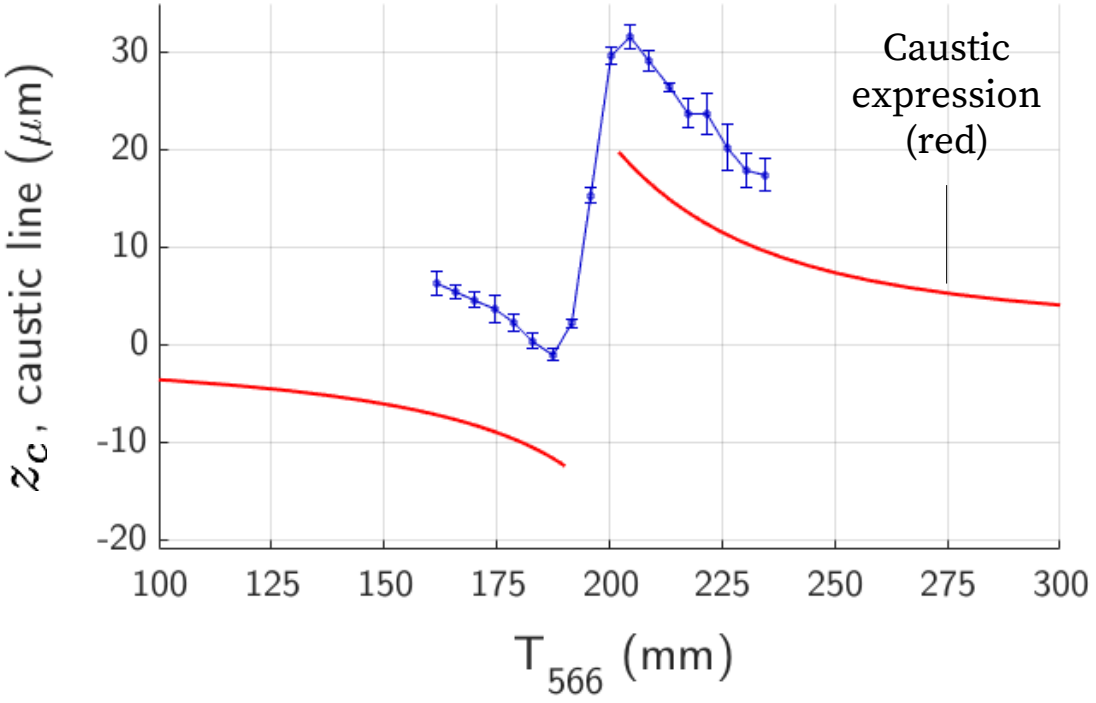

Offset removed

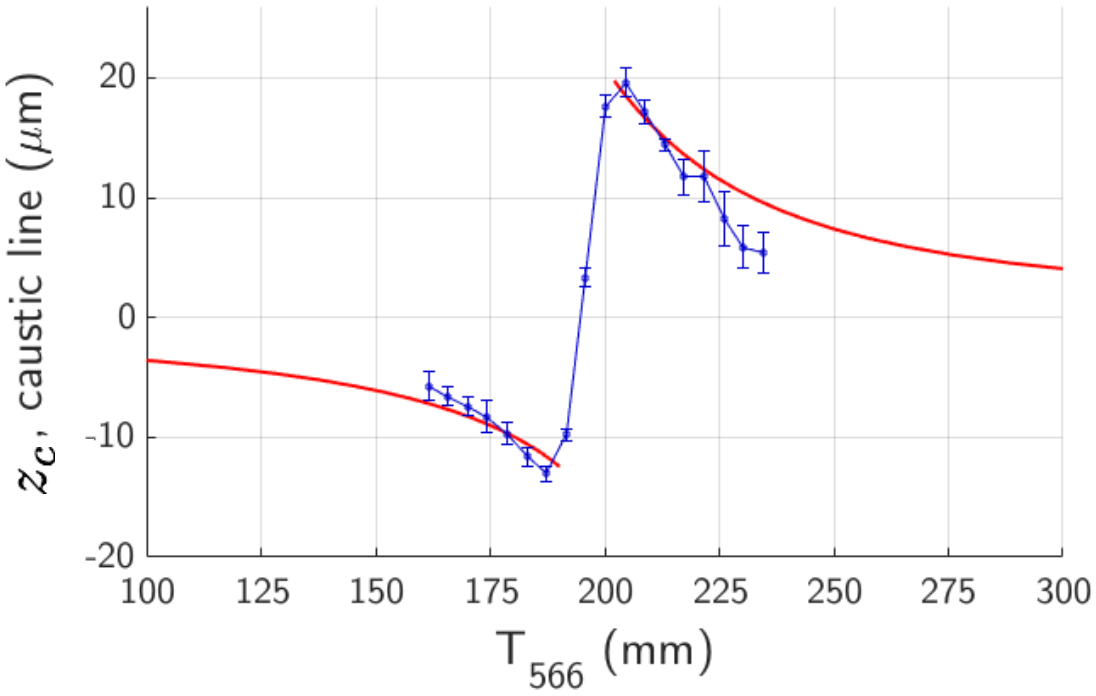

Offset due to the combined effects of wakefields and curvature of the phase space distribution.

Mapping out caustic lines

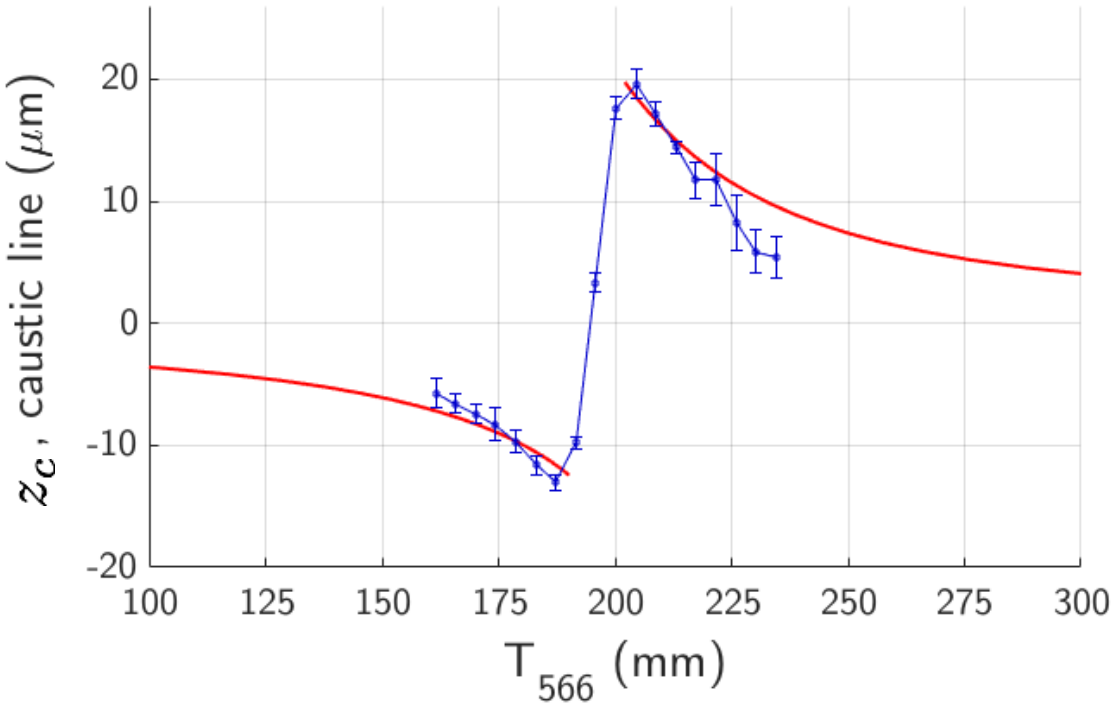

Offset of 14 micrometers removed

Where the caustic expression is undefined, the longitudinal phase space is considered well linearized, resulting in a short bunch with a symmetrical current profile.

$$z_c(z_i) = -z_i - \frac{R_{56}\delta(z_i)}{2} + \frac{U_{5666}\ \delta^3(z_i)}{2} + \frac{\delta(z_i)}{2\delta'(z_i)}$$

$$\tilde{T}_{566}(z_i) = \frac{1}{2\delta(z_i)}\left(-R_{56} - \frac{1}{\delta'(z_i)} - 3U_{5666}\ \delta^2(z_i)\right)$$

T.K.Charles et al. IPAC19, WEYYPLS2

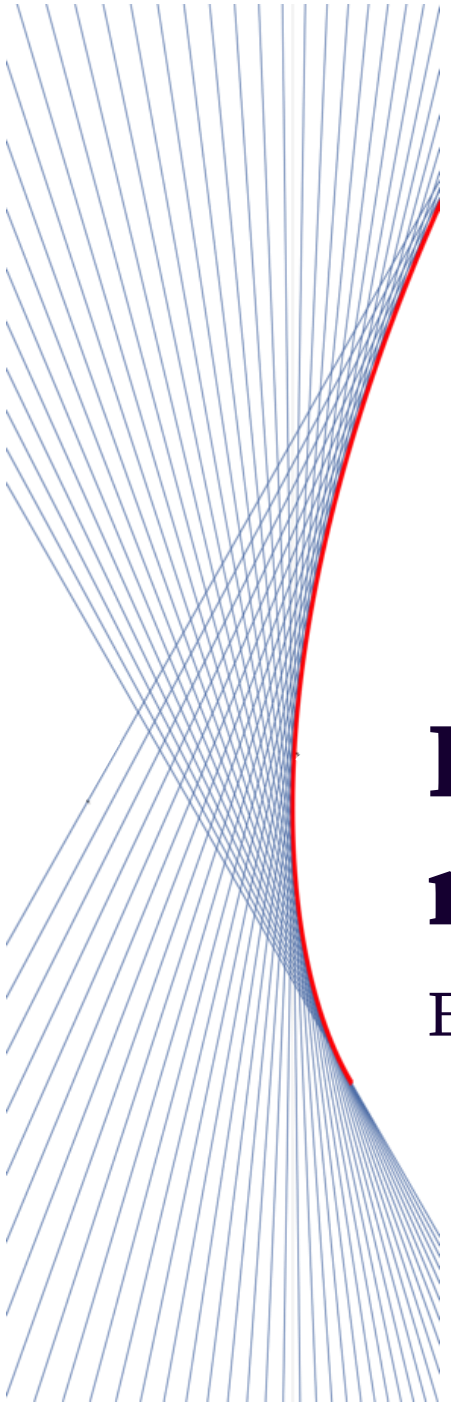

Longitudinal Phase Space manipulation in recirculating machines

Example of the usefulness of caustics

with
Dave Douglas, JLAB
Peter Williams, Cockcroft Institute

A UK recirculating FEL concept

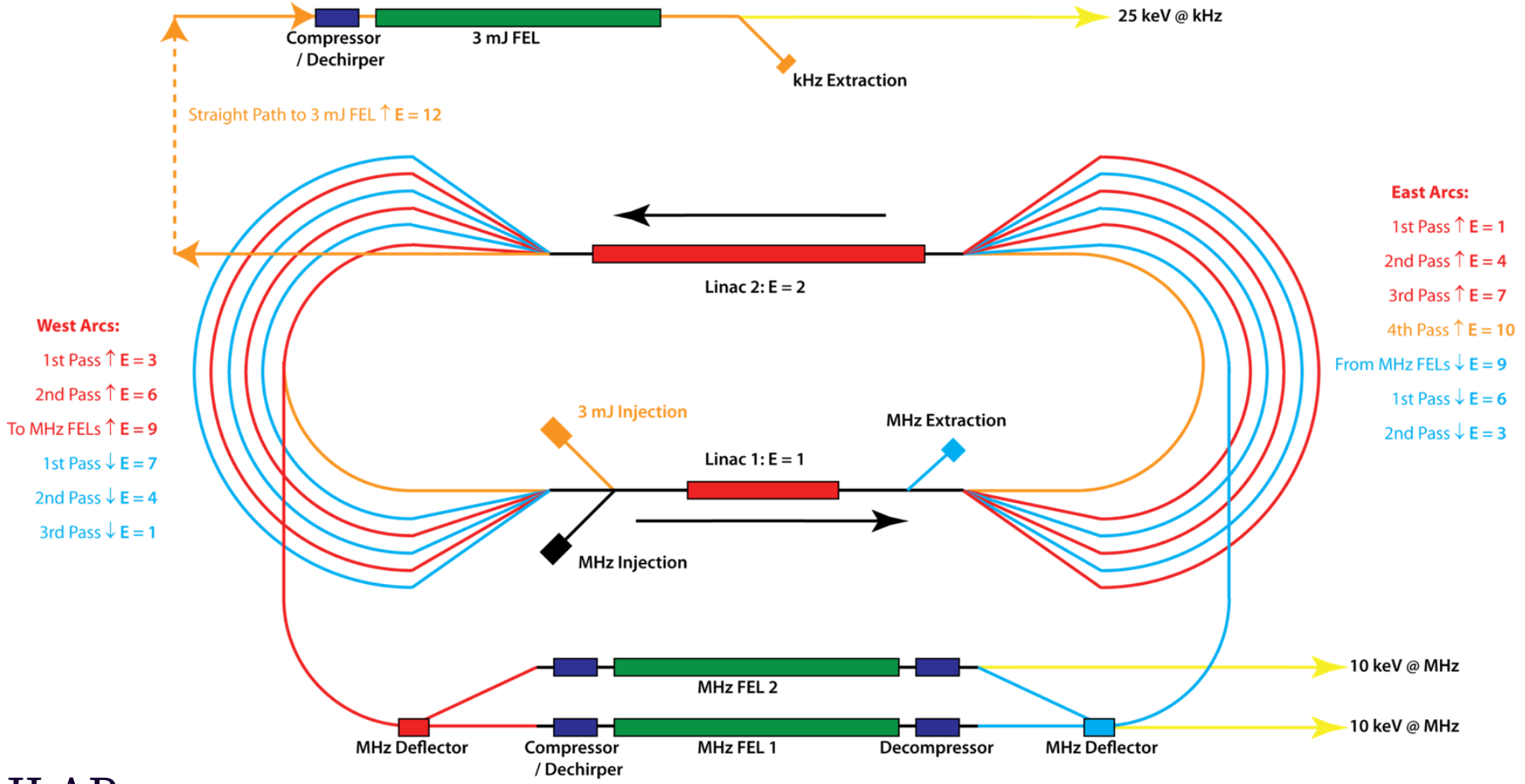

with
Dave Douglas, JLAB
Peter Williams, Cockcroft Institute

Caustic exclusion plots for each arc of a recirculating machine during acceleration

Arc no.

1

2

3

4

5

6

7

8

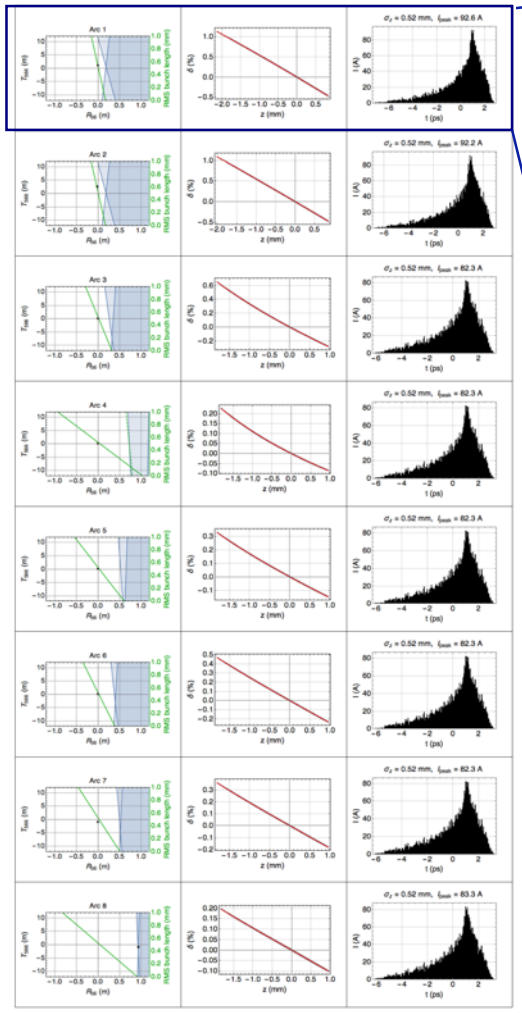

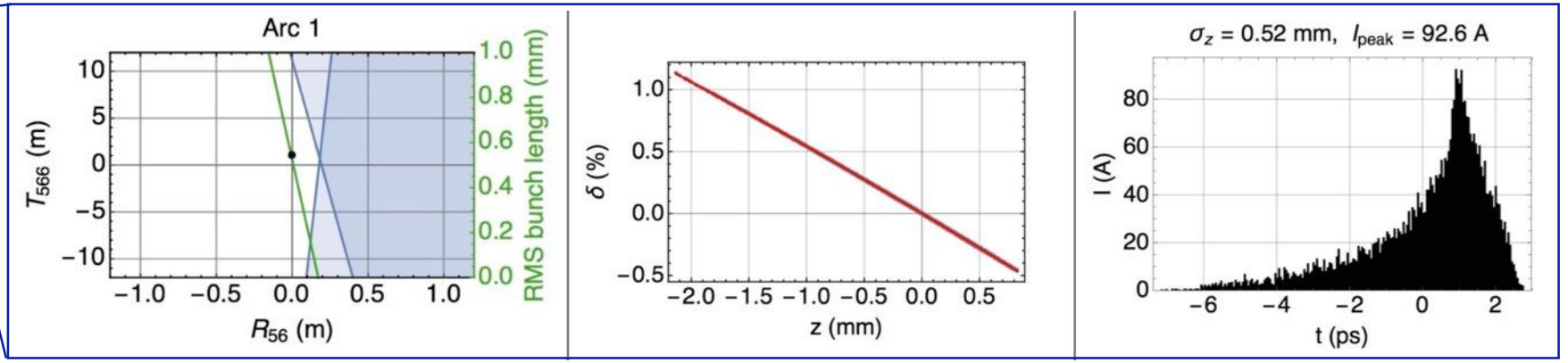

- Non-caustic region
- Region of single fold caustic (single current spike)
- Region of two fold caustics (multiple current spike)

Caustic exclusion plots for each arc of a recirculating machine during acceleration

Arc no.

1

2

3

4

5

6

7

8

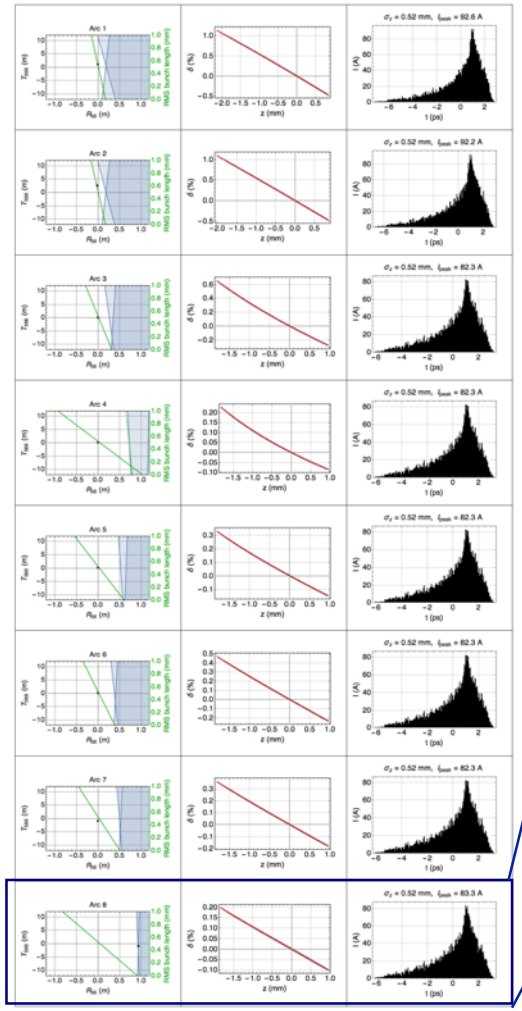

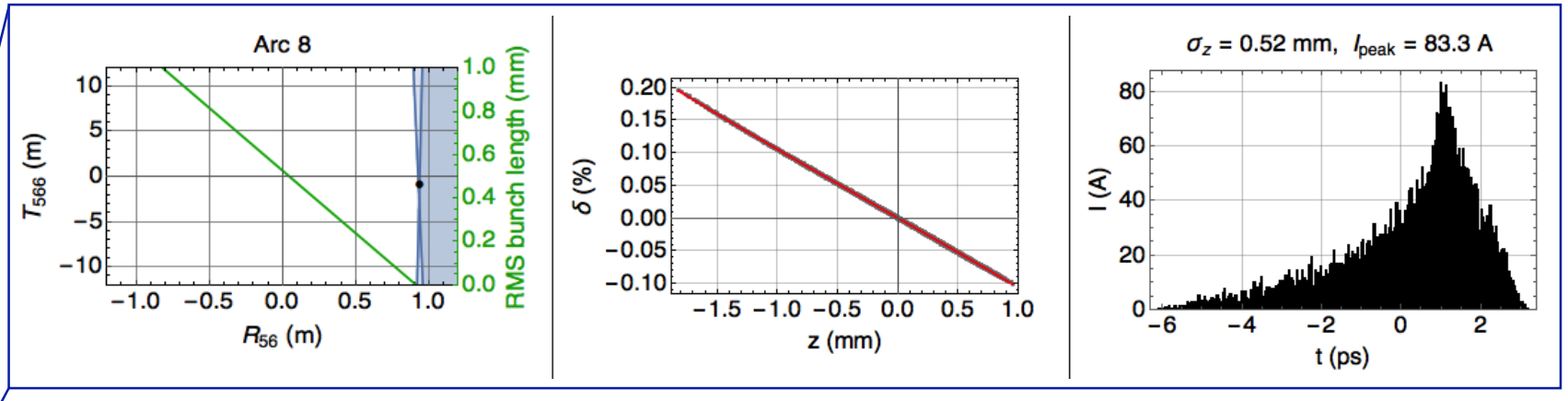

Non-caustic region

Region of single fold caustic (single current spike)

Region of two fold caustics (multiple current spike)

Bunch distributions at various positions around the accelerator

Bunch Distribution from gun:

With thanks to **Julian McKenzie** (Daresbury, UK) for this distribution.

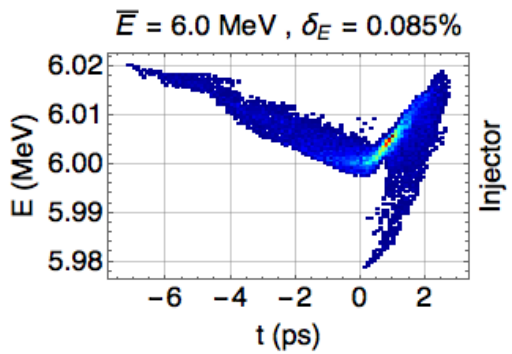

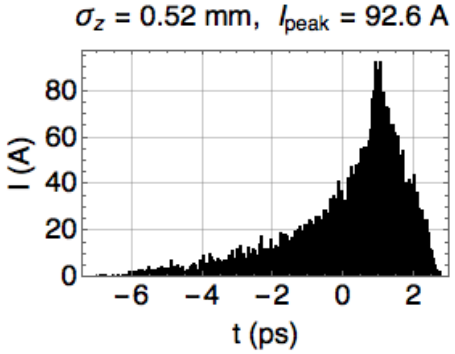

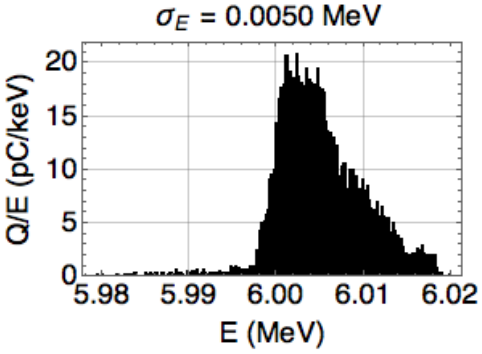

Distribution at end of arc 8:

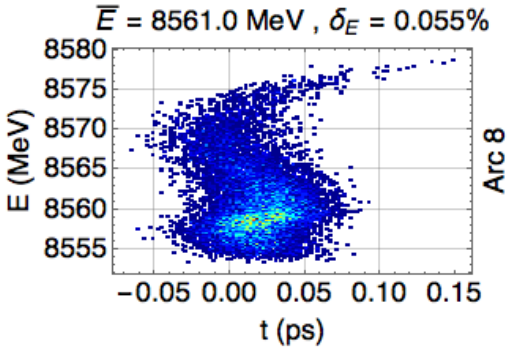

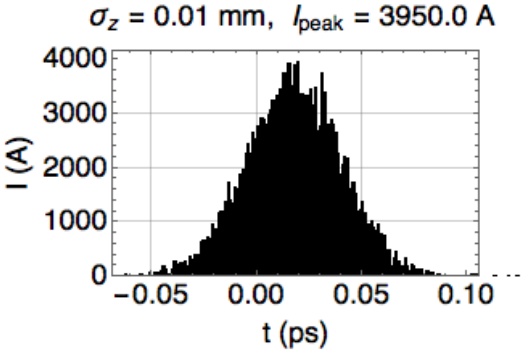

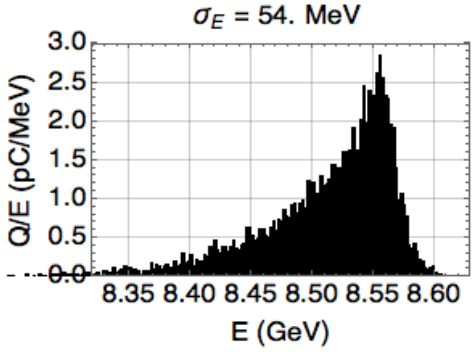

Distribution after lasing:

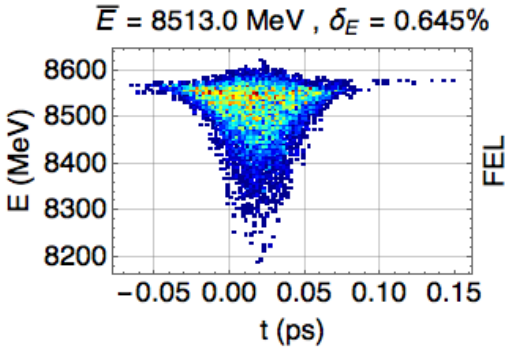

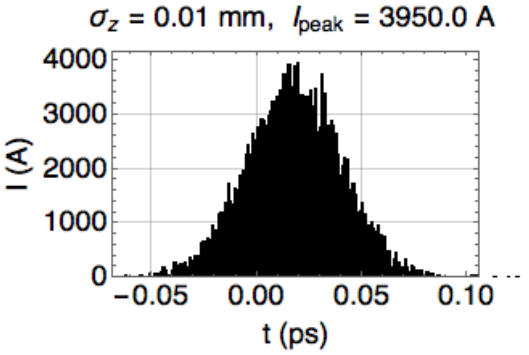

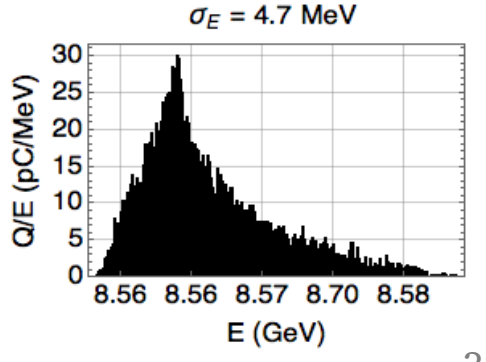

Caustic exclusion plots for each arc of a recirculating machine during deceleration

Arc no.

9

10

11

12

13

14

15

16

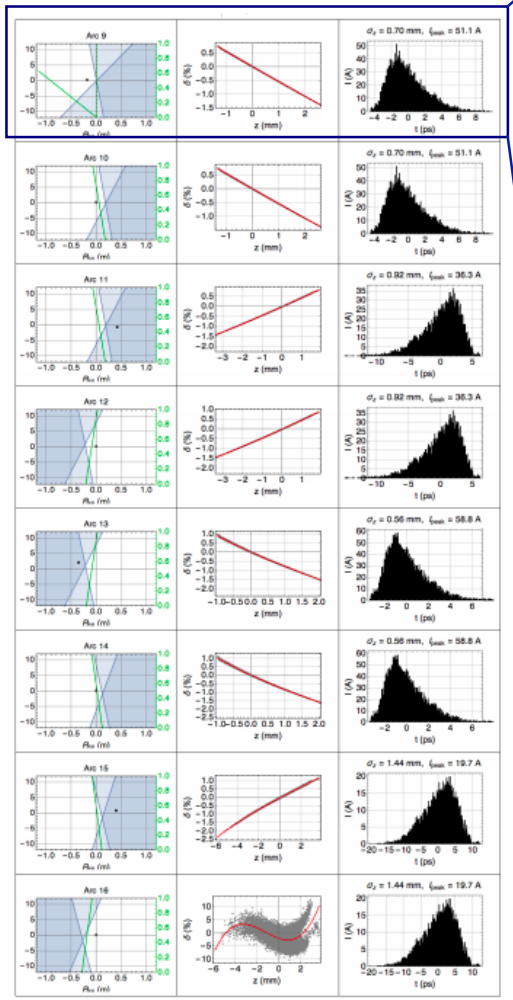

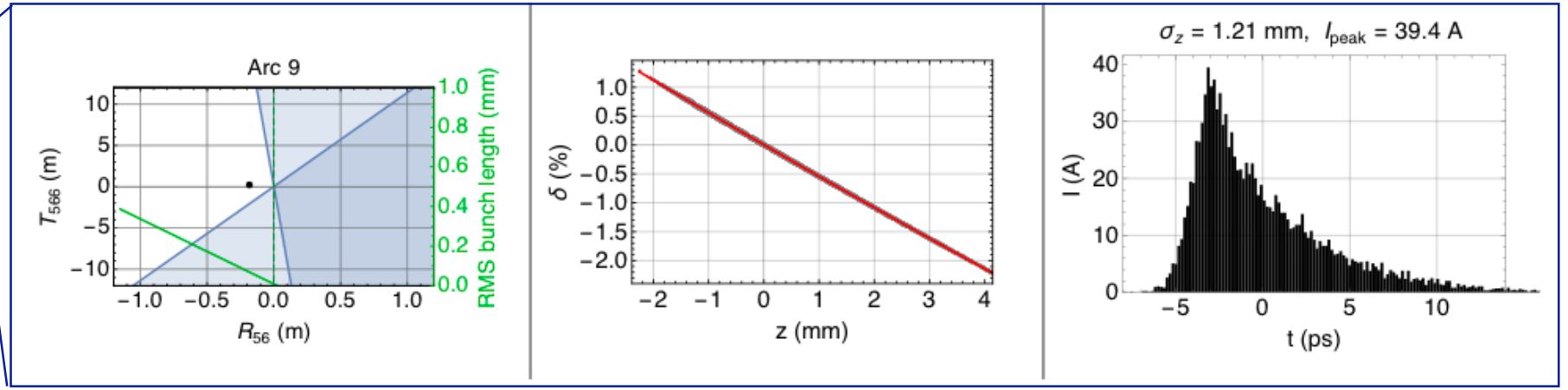

- Non-caustic region
- Region of single fold caustic (single current spike)
- Region of two fold caustics (multiple current spike)

Caustic exclusion plots for each arc of a recirculating machine during deceleration

Arc no.

9

10

11

12

13

14

15

16

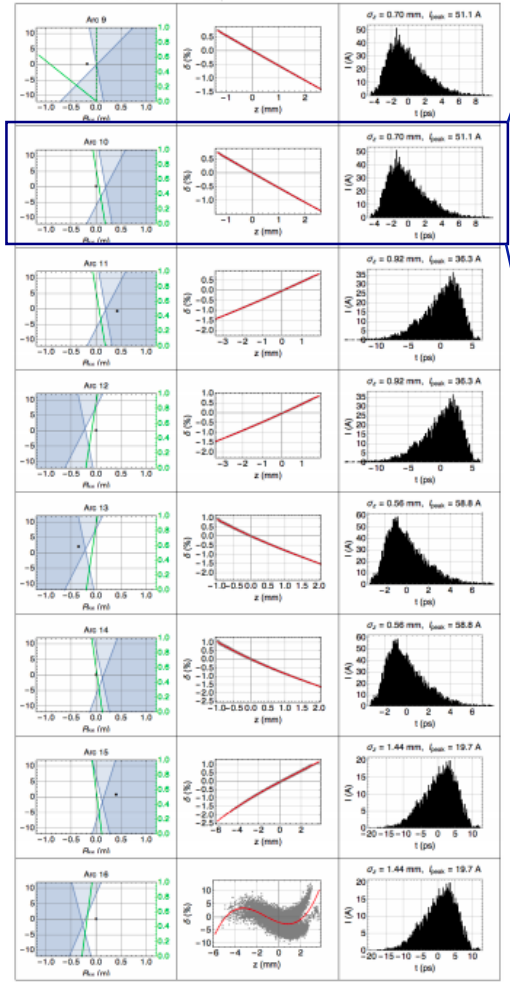

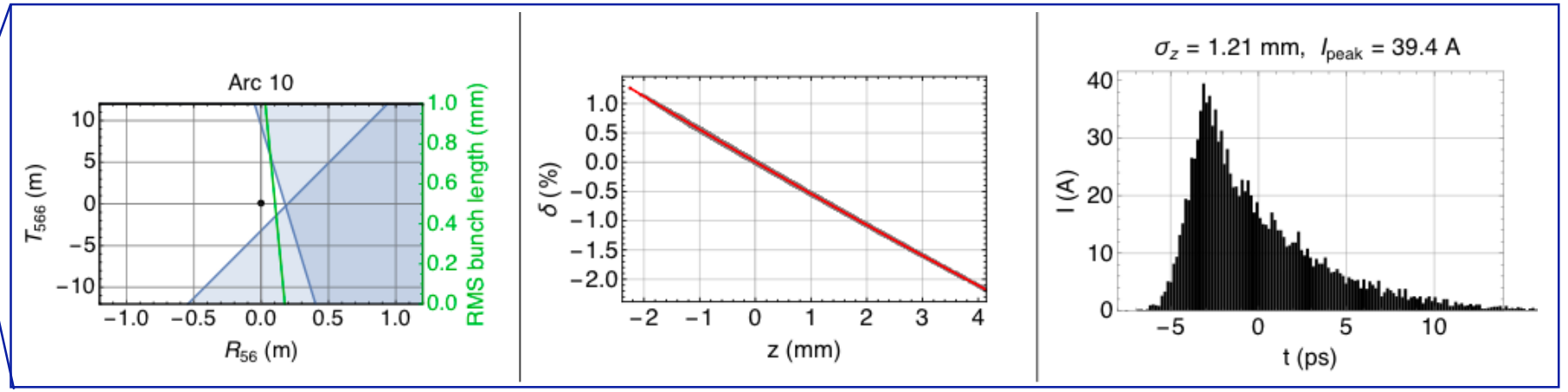

- Non-caustic region
- Region of single fold caustic (single current spike)
- Region of two fold caustics (multiple current spike)

Caustic exclusion plots for each arc of a recirculating machine during deceleration

Arc no.

9

10

11

12

13

14

15

16

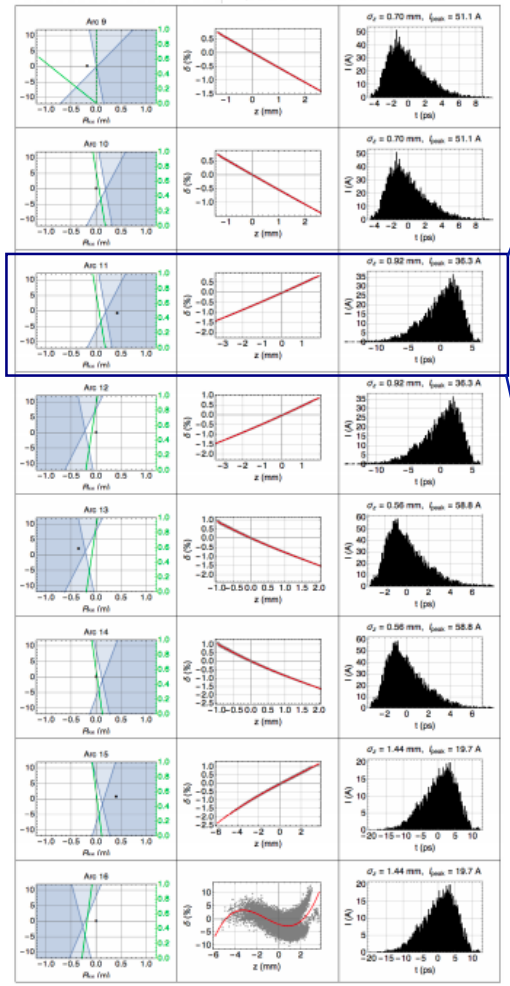

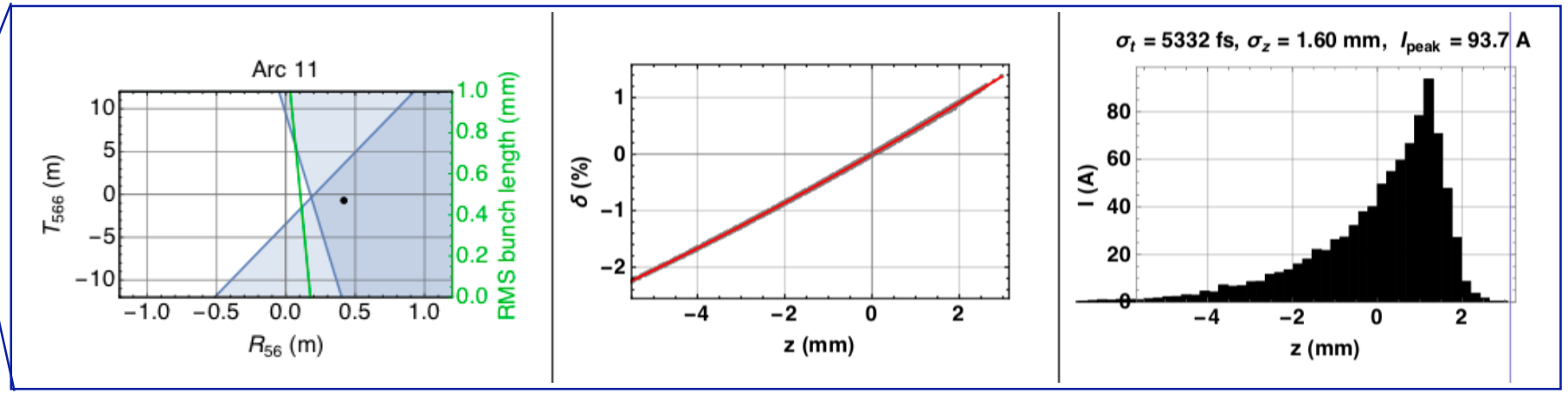

- Non-caustic region
- Region of single fold caustic (single current spike)
- Region of two fold caustics (multiple current spike)

Caustic exclusion plots for each arc of a recirculating machine during deceleration

Arc no.

9

10

11

12

13

14

15

16

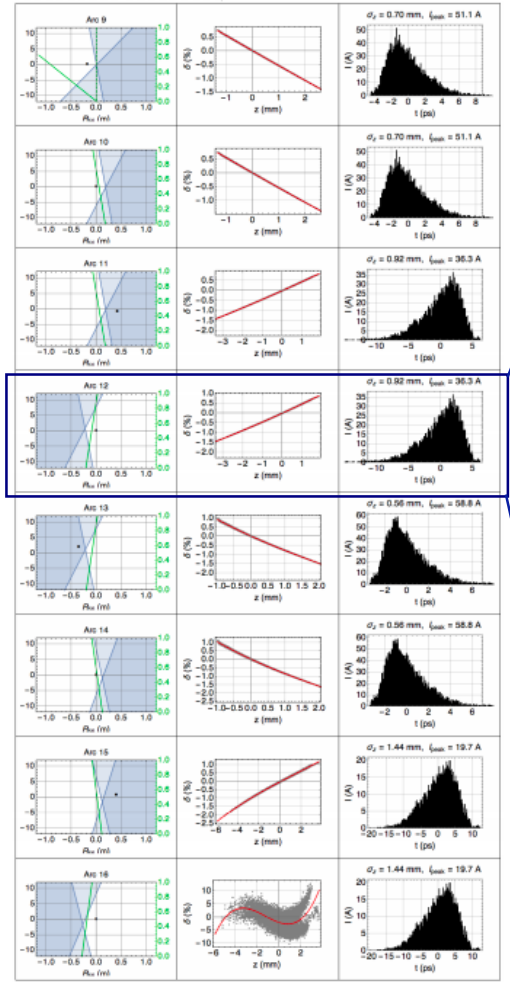

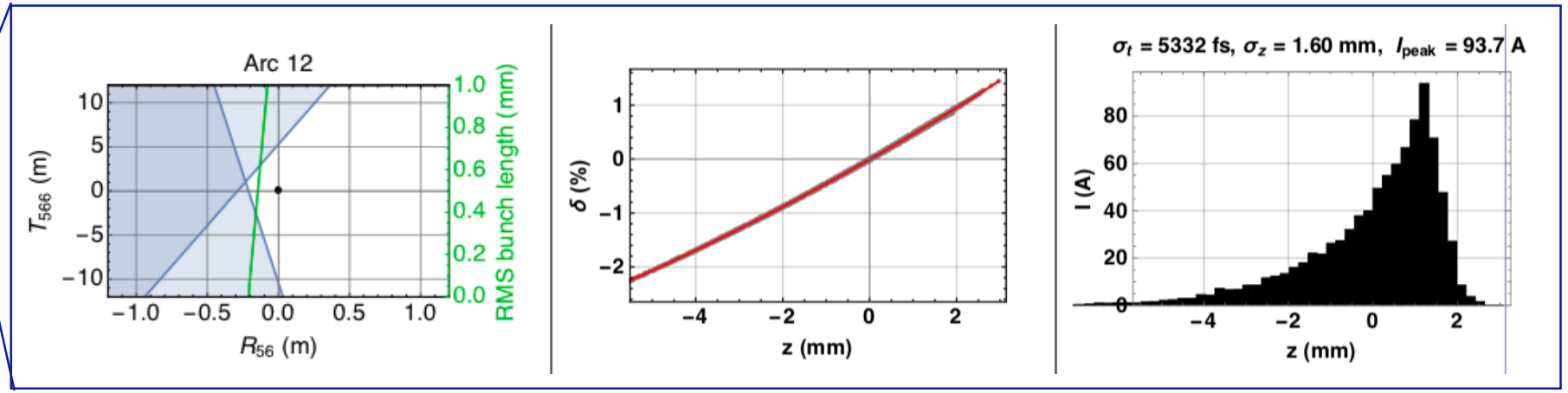

- Non-caustic region
- Region of single fold caustic (single current spike)
- Region of two fold caustics (multiple current spike)

Bunch distributions at various positions around the accelerator

Distribution after lasing:

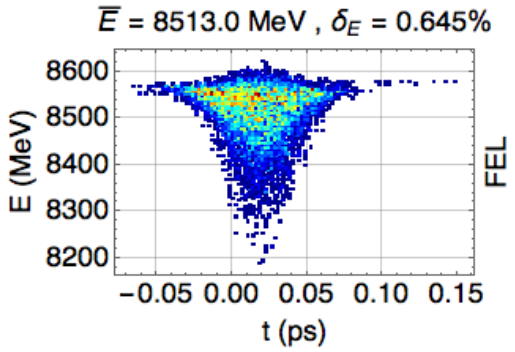

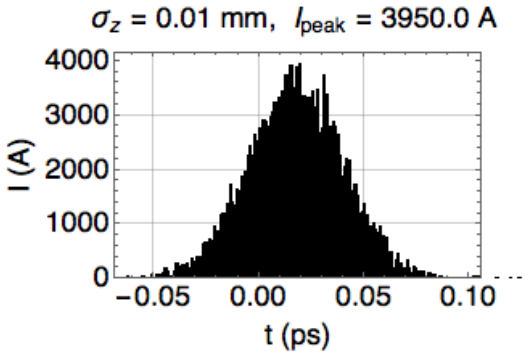

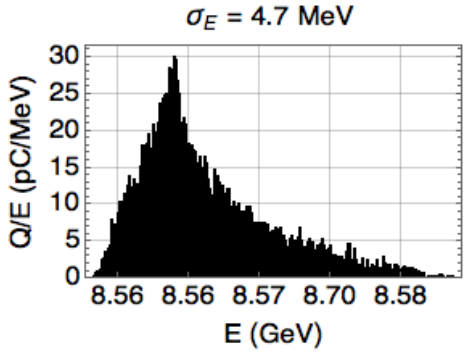

Distribution at dump:

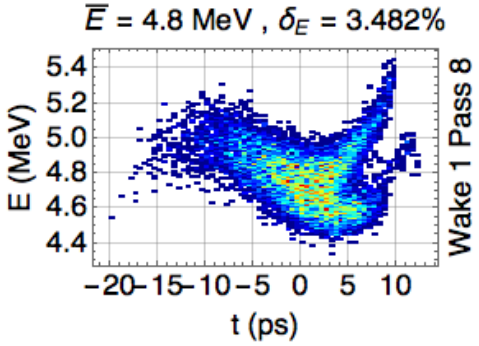

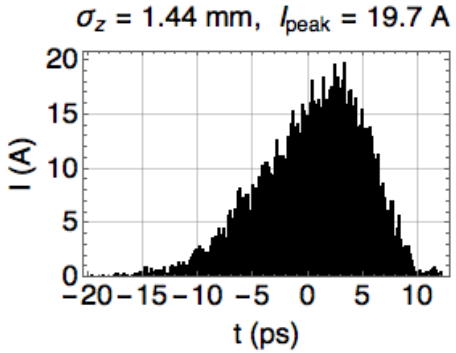

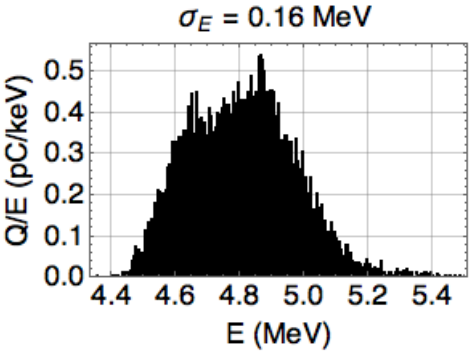

T.K.Charles et al. IPAC18, WEYGBE2

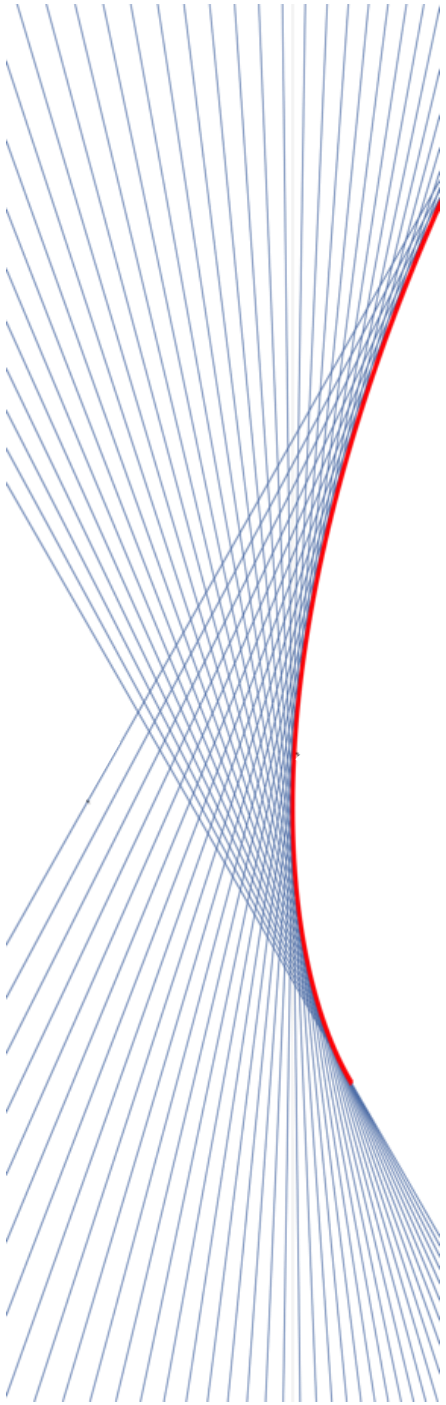

Microbunching instability

Example of caustics

Micro-bunching caustics

A caustic expression can also be derived for micro-bunching. Each line shows where a current spike will be seen.

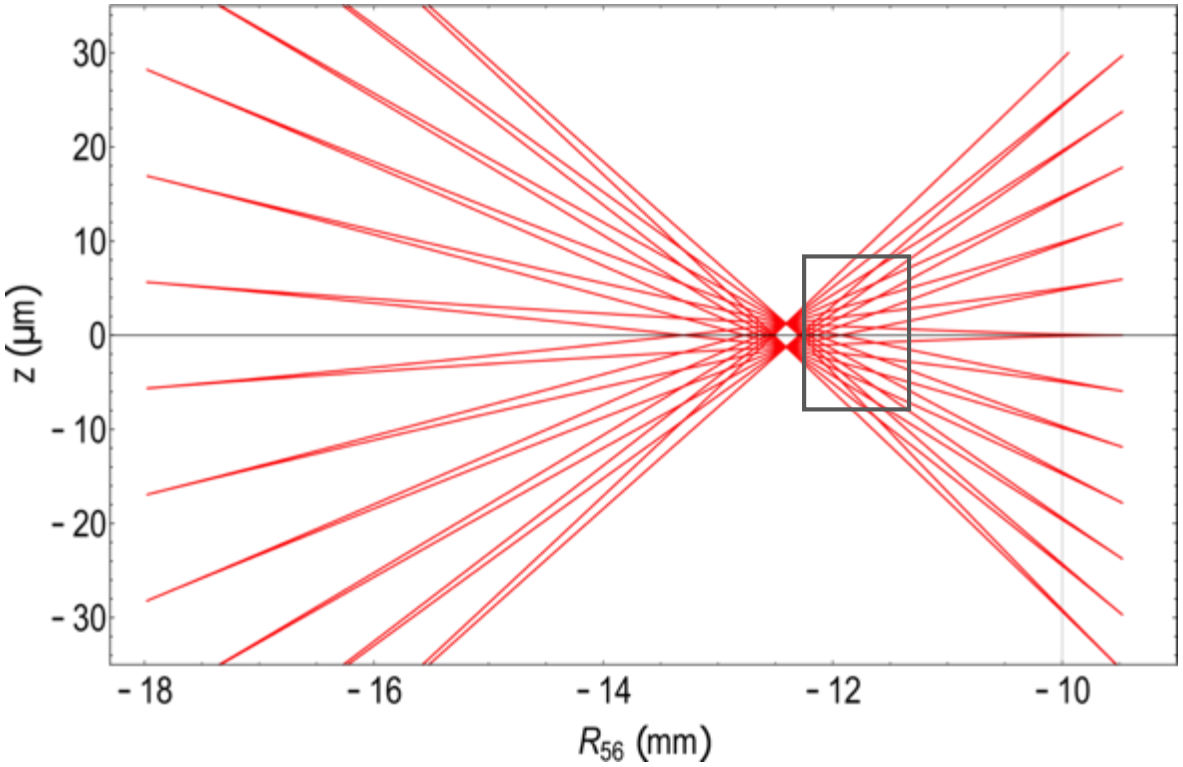

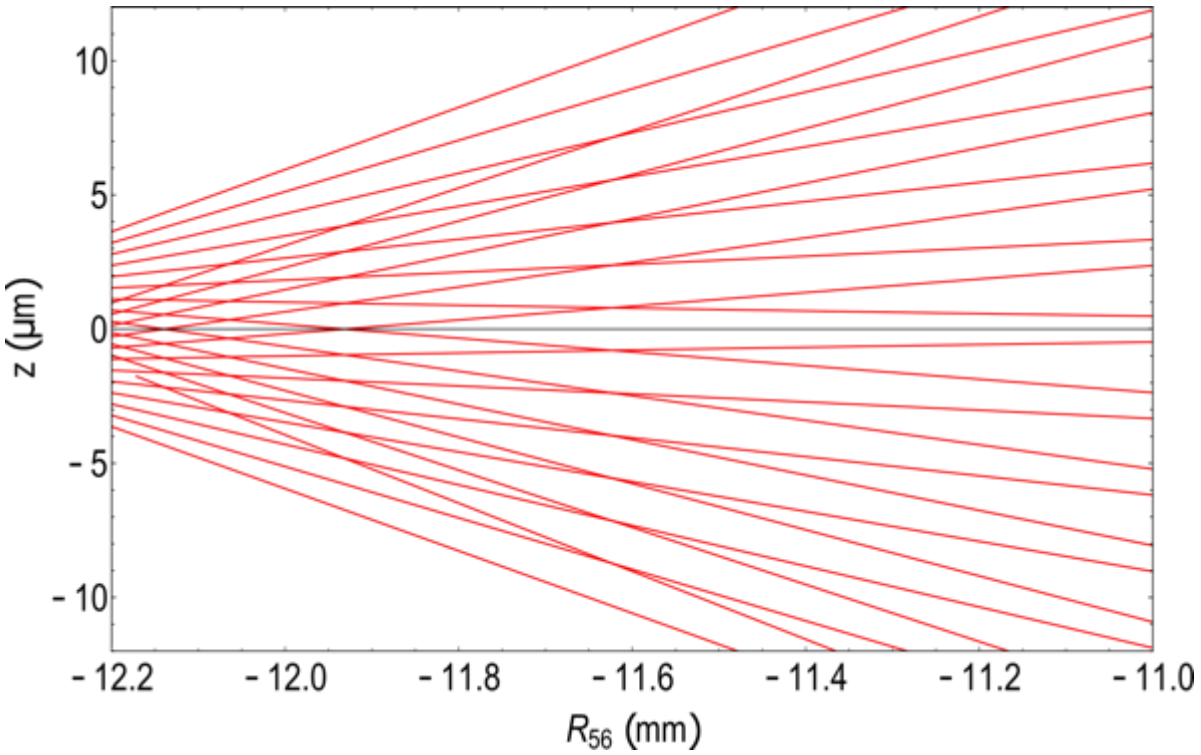

Caustic nature leads to bifurcated current peaks

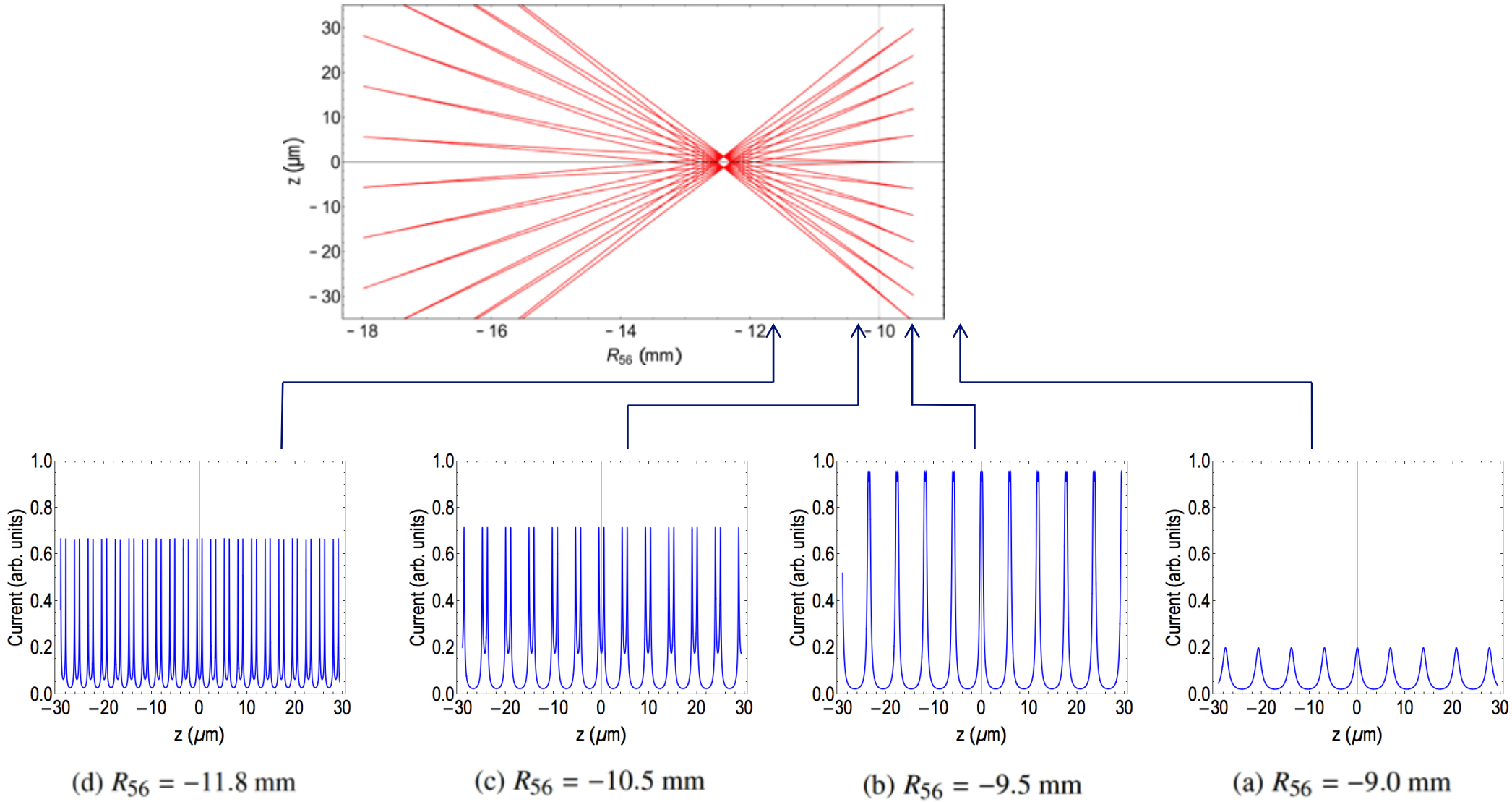

(d) $R_{56} = -11.8$ mm (c) $R_{56} = -10.5$ mm (b) $R_{56} = -9.5$ mm (a) $R_{56} = -9.0$ mm

Micro-bunching with higher-order effects

Hyper-caustics *'caustics of caustics'*

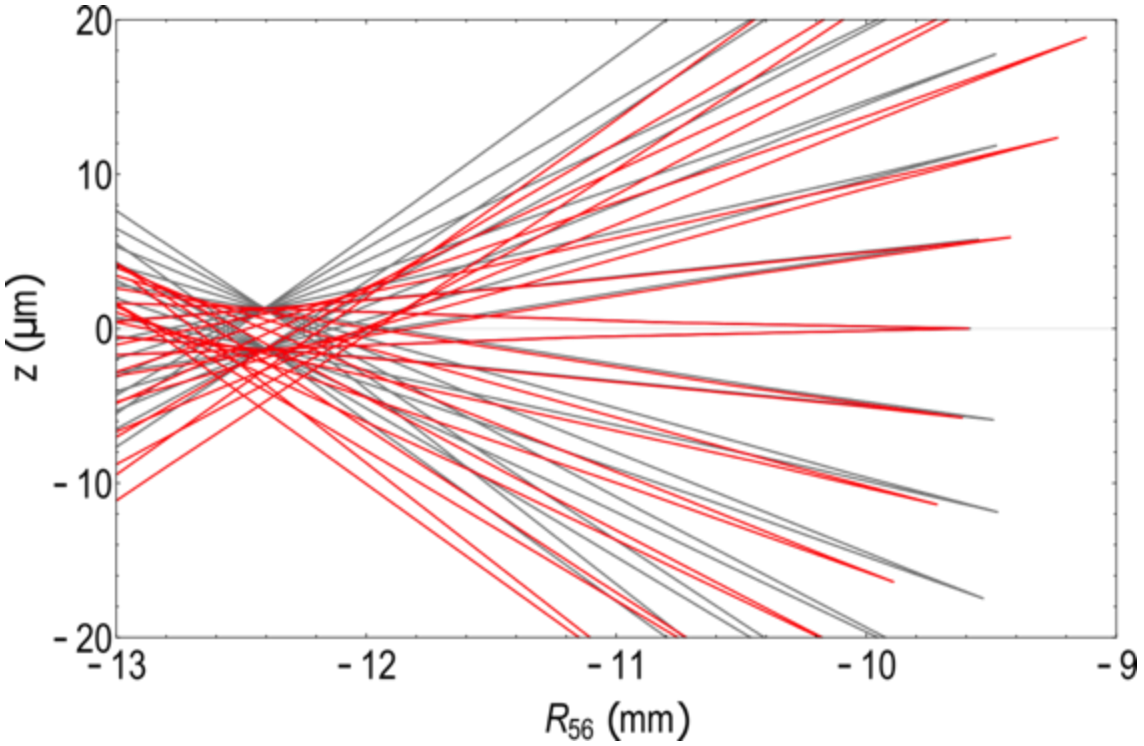

grey: T_{566} = 0, U_{5666} = 0 mm

red: T_{566} = -30 mm, U_{5666} = 0 mm

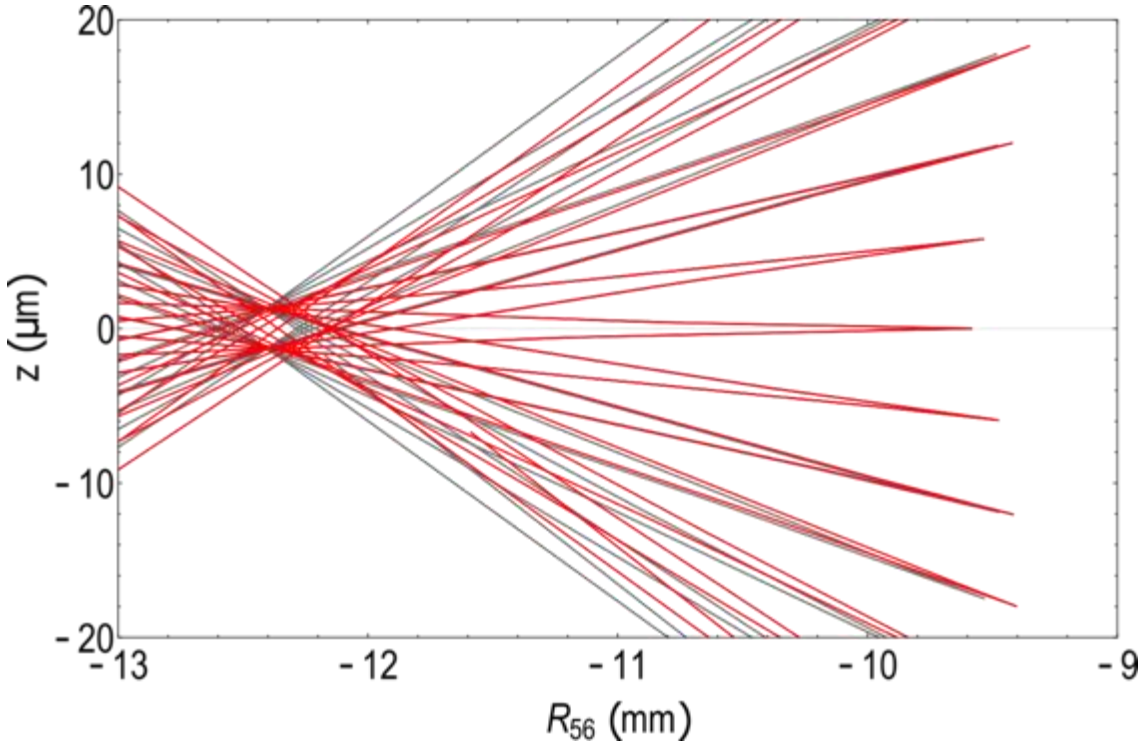

grey: T_{566} = 0, U_{5666} = 0 mm

red: T_{566} = 0, U_{5666} = -2 m

CSR with microbunching

$$\frac{dE}{cdt} = \frac{-2e^2}{4\pi\epsilon_0(3R^2)^{1/3}} \int_{\tilde{z}-z_L}^{\tilde{z}} \frac{d\lambda}{dz} \left(\frac{1}{\tilde{z}-z}\right)^{1/3} dz$$

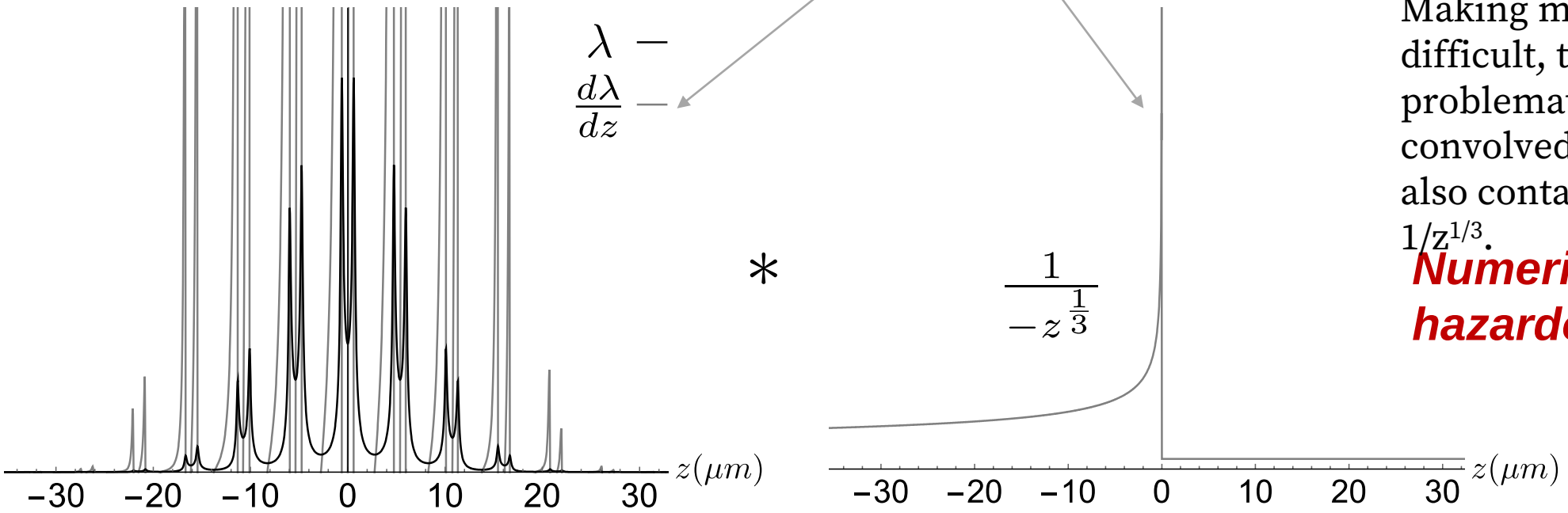

The caustic nature of microbunching results in sharp peaks in the linear charge density function, λ(z), which means the numerical evaluation of dλ/dz is risky. Making matters even more difficult, this numerically problematic data set is then convolved with a function that also contains a singularity, $1/z^{1/3}$.

Numerically hazardous!

Conclusions …

Caustics are a useful way that we can look at various types of focusing.

Caustics are commonplace in optics, they are ultilised in electron microscopy, and they are also seen in accelerator physics.

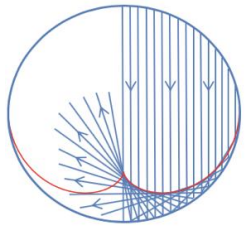

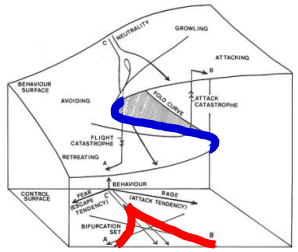

Applied to accelerator physics, we can explore the high-order focusing.

$$\tilde{z}_c(z_i) = z_i + \frac{\delta(z_i)(-1 + T_{566}(-2+\delta(z_i))\delta'(z_i) + U_{5666}(-3+\delta(z_i)^2)\delta'(z_i))}{\delta'(z_i)}$$

$$\tilde{R}_{56}(z_i) = \frac{-1 - 2T_{566}\delta'(z_i) - 3U_{5666}\delta'(z_i)}{\delta'(z_i)}$$

Fold

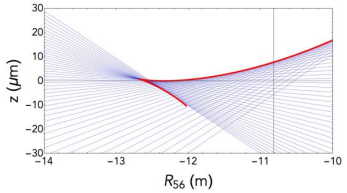

Cusp

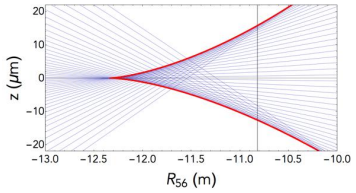

Butterfly

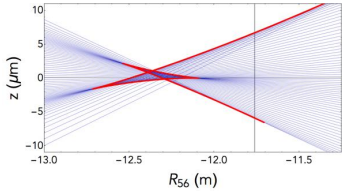

Phys. Rev. Accel. Beams, (2016) **19**, 104402

Current horns (often seen in FELs) can be suppressed by considering the underlying caustics, resulting in 63% reduction in the CSR-induced emittance growth.

Without octupole:

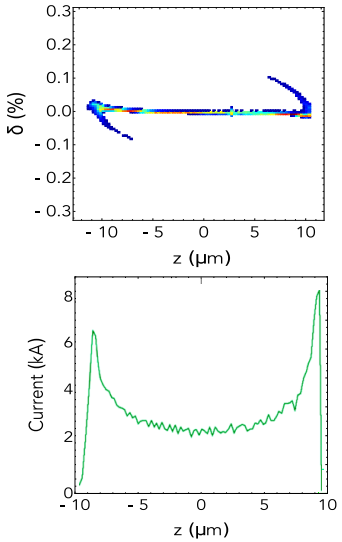

$\epsilon_{nx} = 1.359$ mm mrad

With octupole:

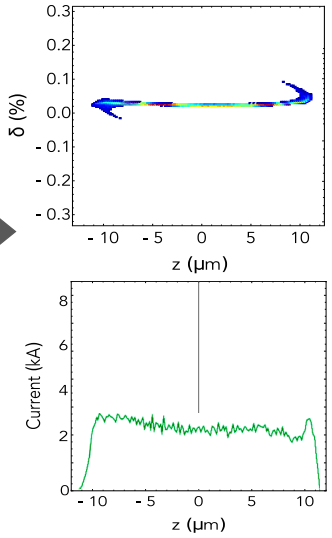

$\epsilon_{nx} = 0.762$ mm mrad

Phys. Rev. Accel. Beams, (2017) **20**, 030705

Conclusions

Caustics are a useful way that we can look at various types of focusing.

Longitudinal phase space manipulation in recirculating & energy recovery machines

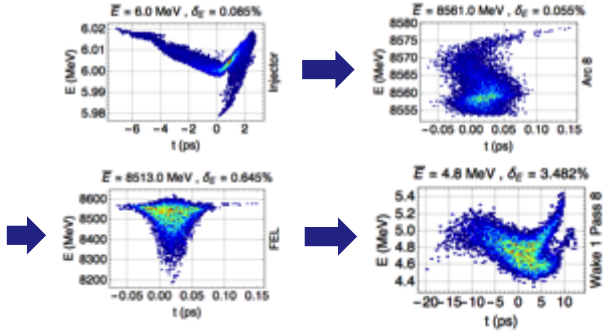

Caustic exclusion plots can be used to pair down viable parameter space.

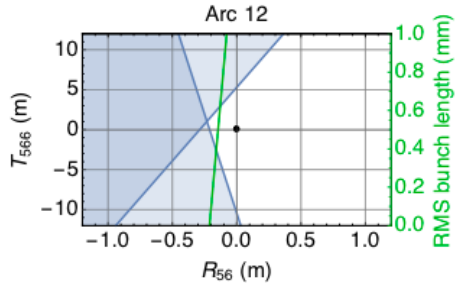

Exclusion plots identify regions where caustics of different codimension exist

IPAC18, WEYGBE2

Experimental demonstration of linearly-ramped current profiles and caustics!

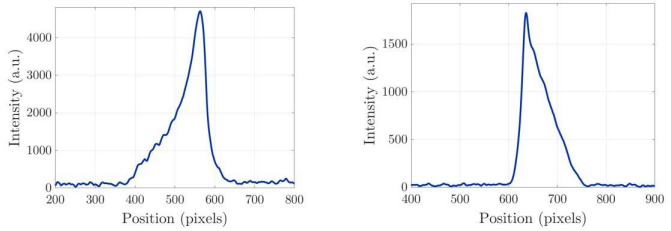

Linearly-ramped current profile achieved through T566 variation.

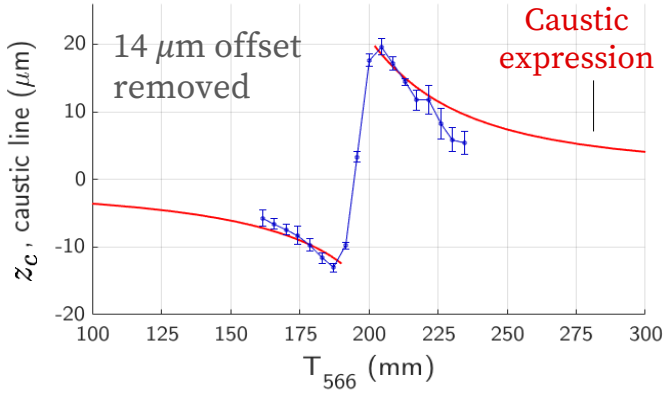

IPAC19, WEYYPLS2

Microbunching is also a caustic phenomenon and can be used to better model microbunching.

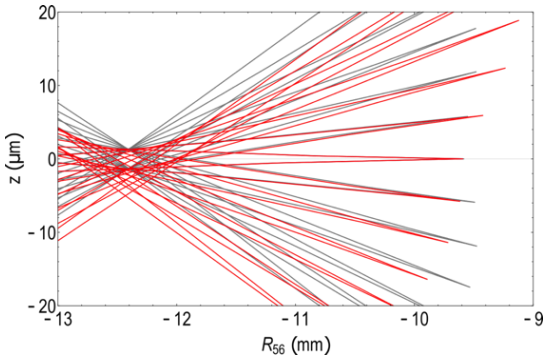

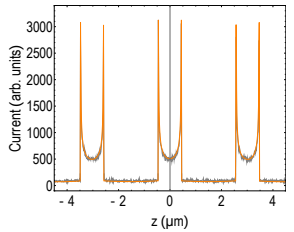

Bifurcated current peaks

Acknowledgements

With acknowledgments and thanks to the people who have supported and contributed to this work:

- Sara Thorin and Jonas Bjorklund Svensson (MAX IV)
- Andrea Latina and Frank Zimmermann (CERN)
- Rohan Dowd (Australian Synchrotron)
- David Paganin (Monash University)
- Mark Boland (Canadian Light Source)
- Peter Williams (Daresbury Laboratory)
- Dave Douglas (J-Lab)

Thank you

Back up slides

Final bunch slice properties

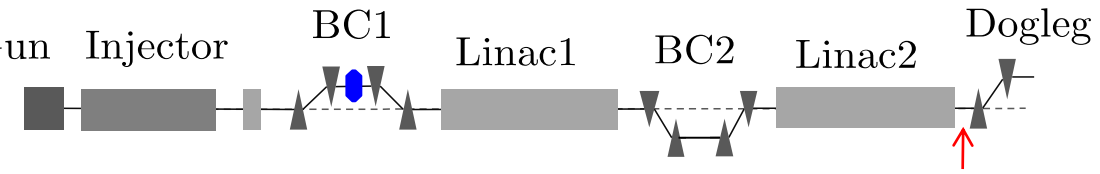

Without octupole: *

With octupole: •

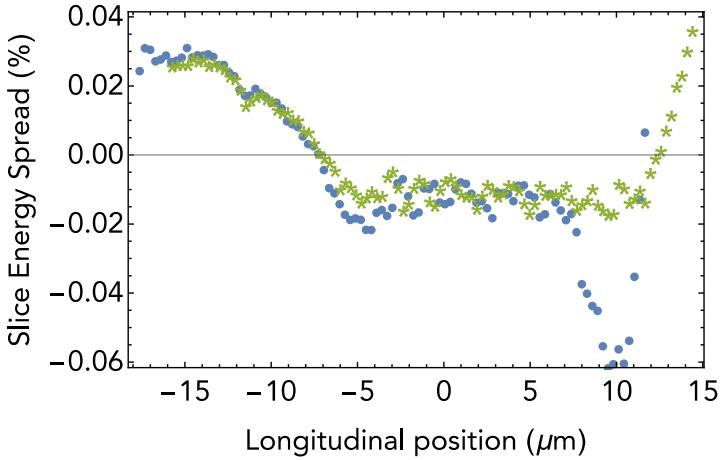

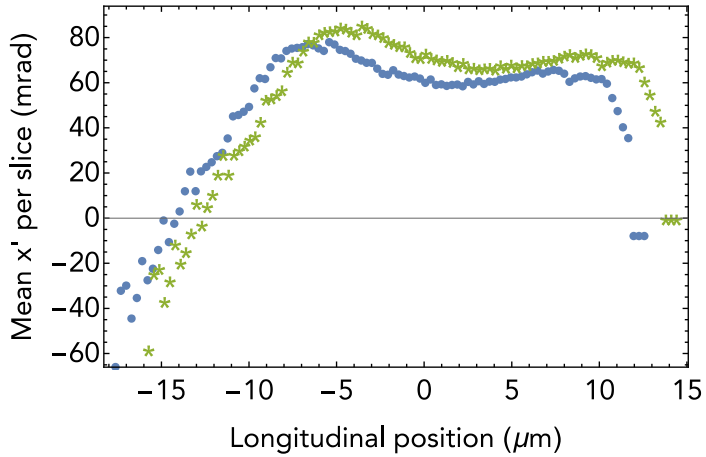

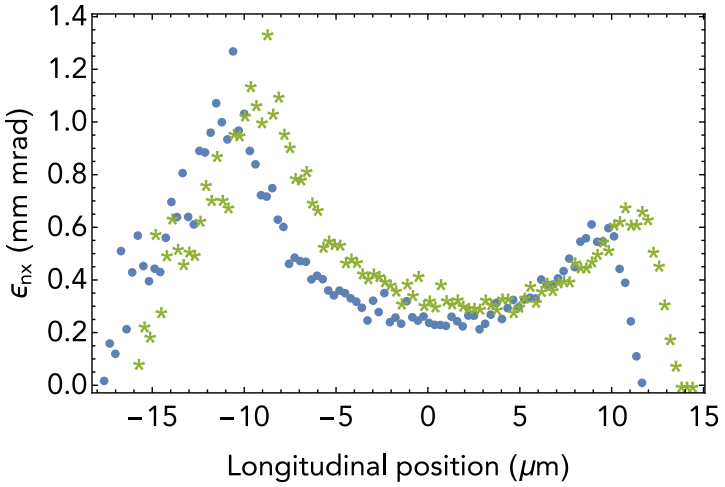

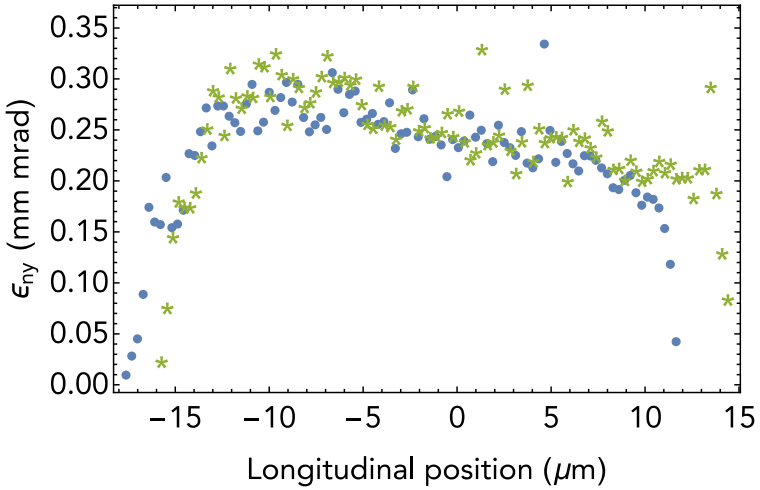

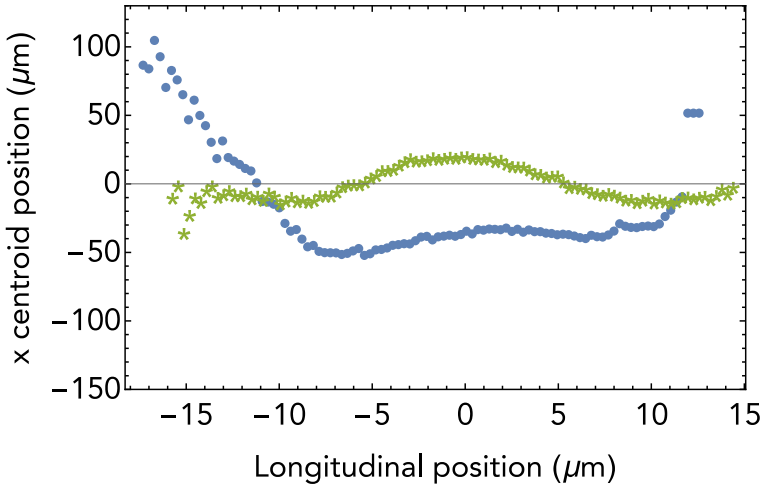

What about chromatic and geometric aberrations?

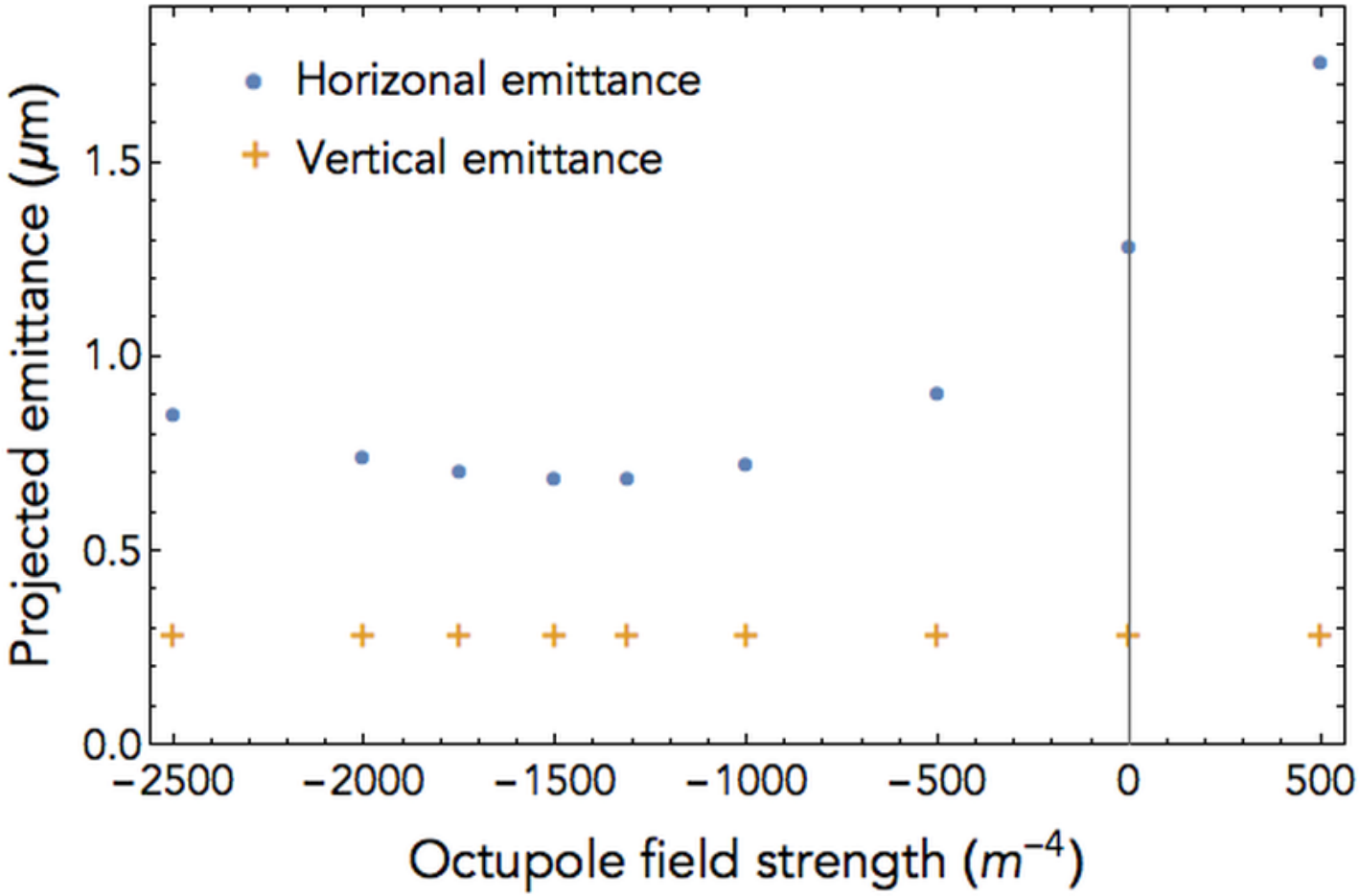

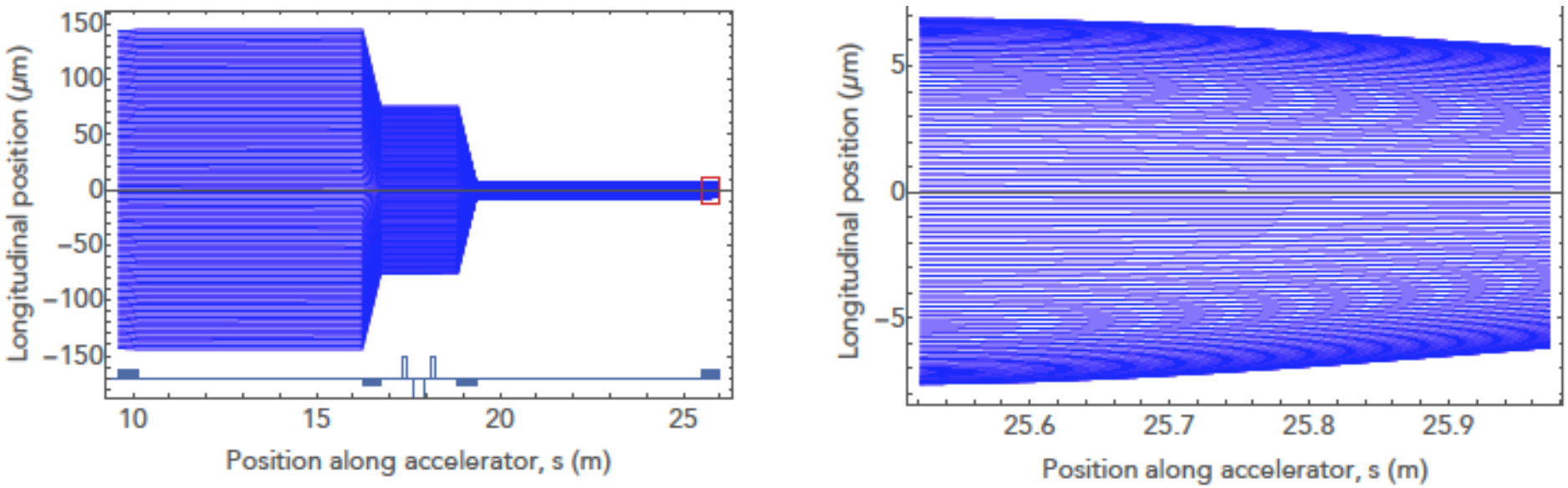

Figure 6.8: Electron trajectories (in s–z space) through a bunch compressor. (b) shows a close up of the trajectories through the fourth dipole (i.e. region outlined with a red box in (a)). Caustics can be seen forming at head and tail of the bunch in (b).

MAX IV Bunch Compressors

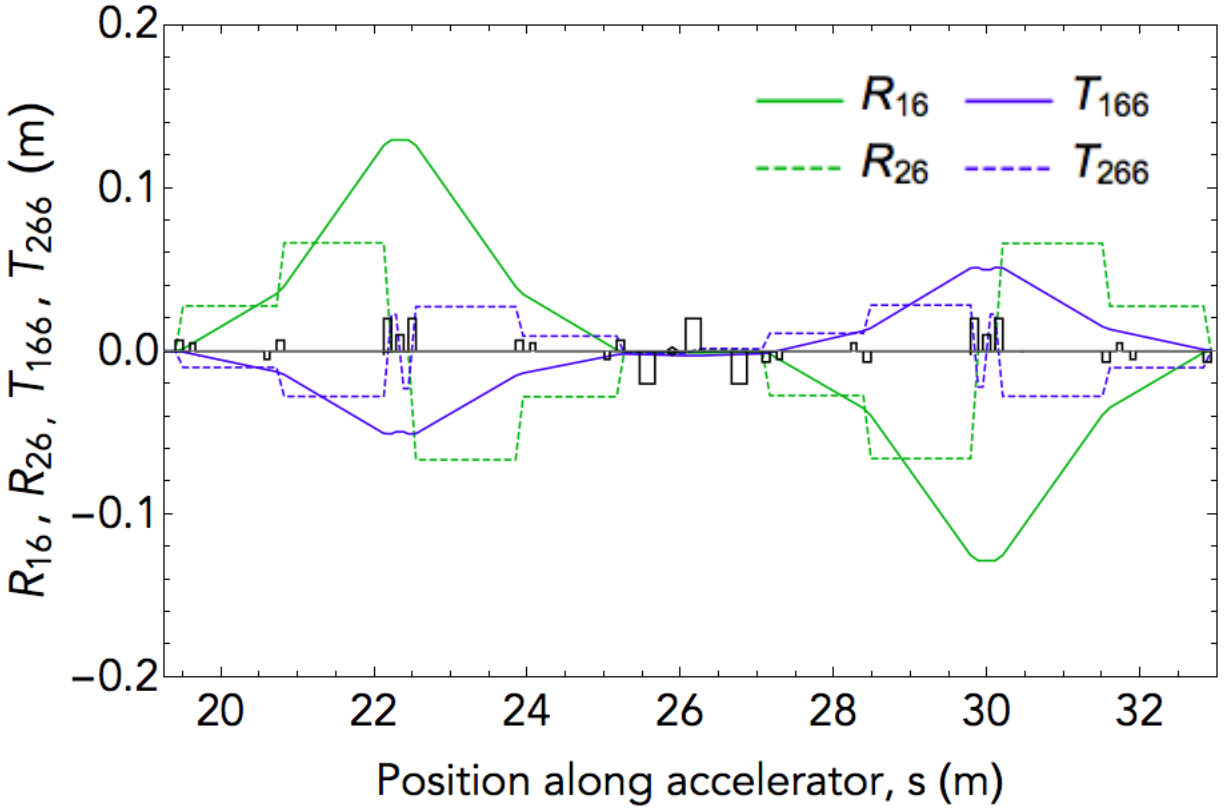

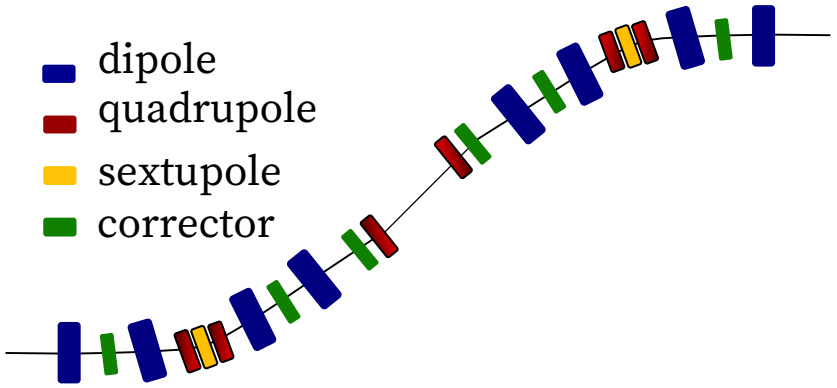

Illustration of compressed bunches

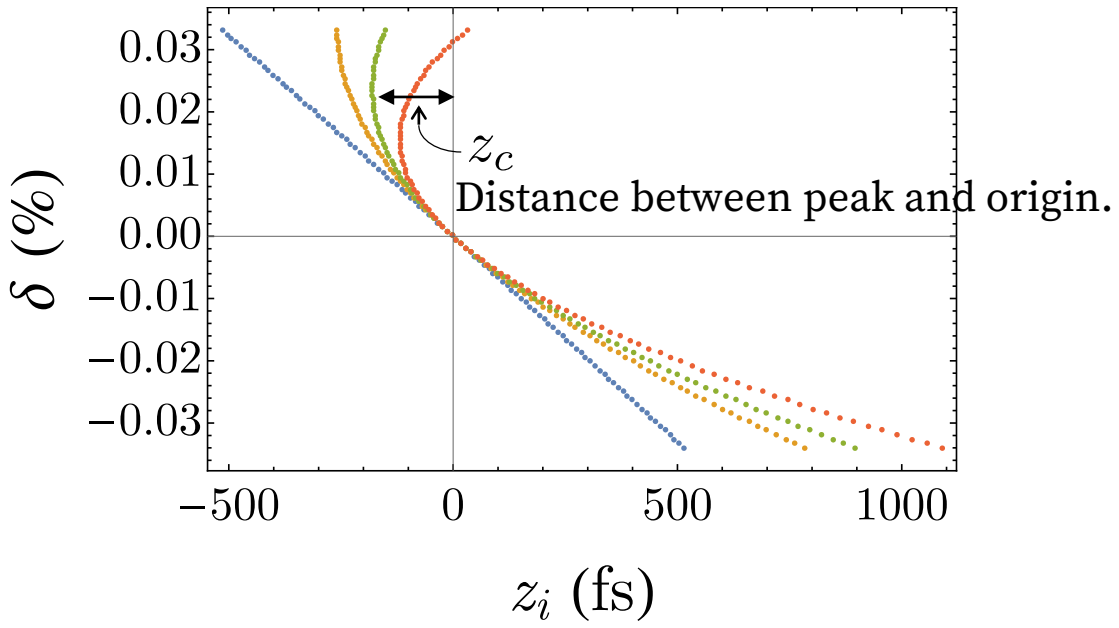

The origin is found as being the distance from one bunch edge to half of the accumulated charge,

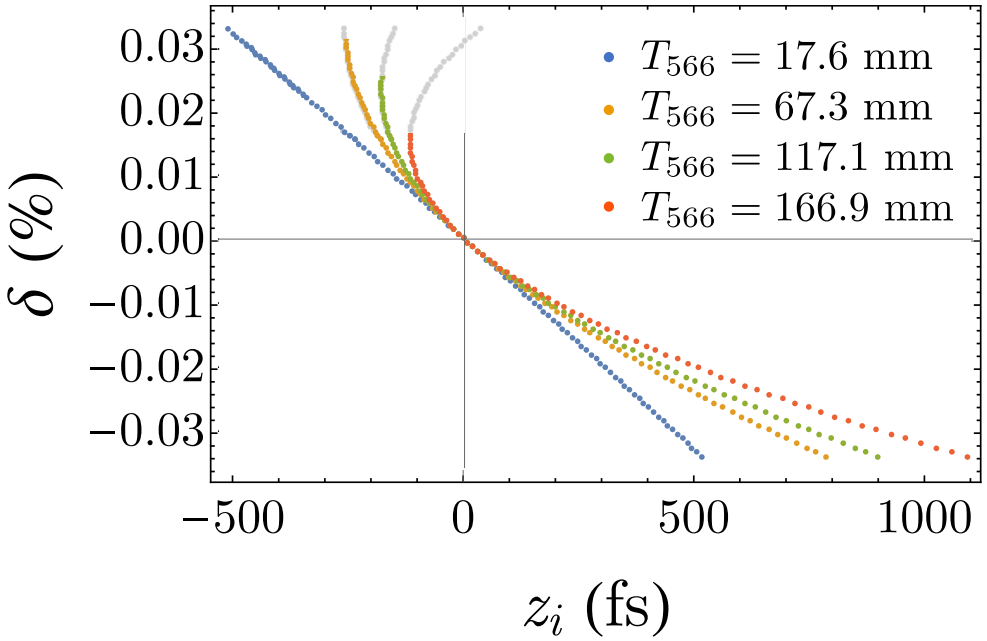

The light grey portion of the distribution will be mapped to a smaller x value, lengthening out the bunch on the screen.

Current profile analytical expression

$$\lambda(z) = \frac{e^{-\frac{z^2}{2\sigma^2}}}{\sqrt{2\pi}\sigma} \frac{f}{1 + R_{56}\delta'(z) + T_{566}\delta''(z) + U_{5666}\delta'''(z)}, \qquad \text{where } f \text{ is a scaling factor.}$$

non-caustic region

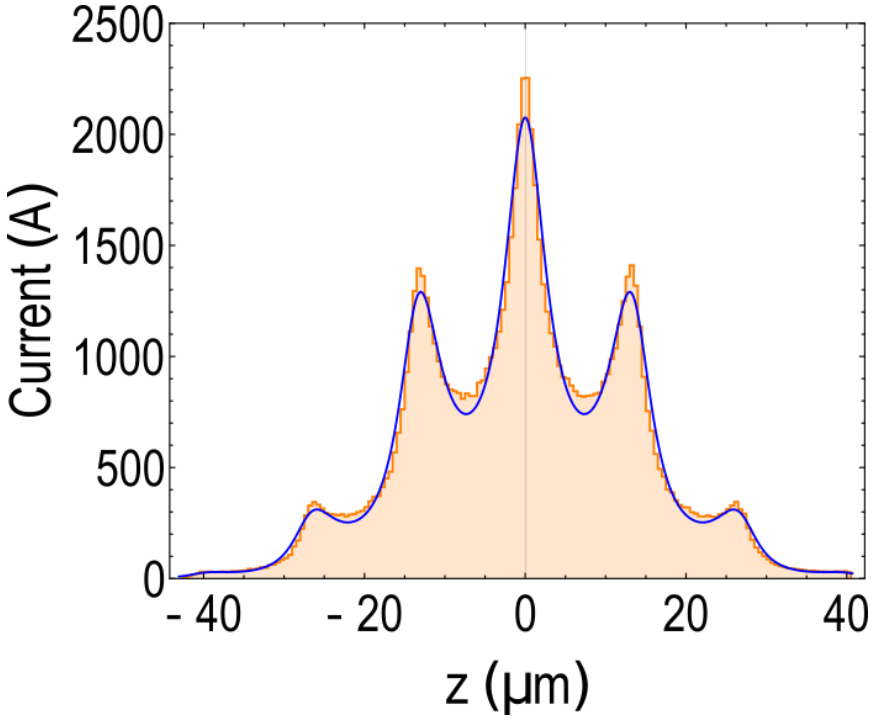

caustic region

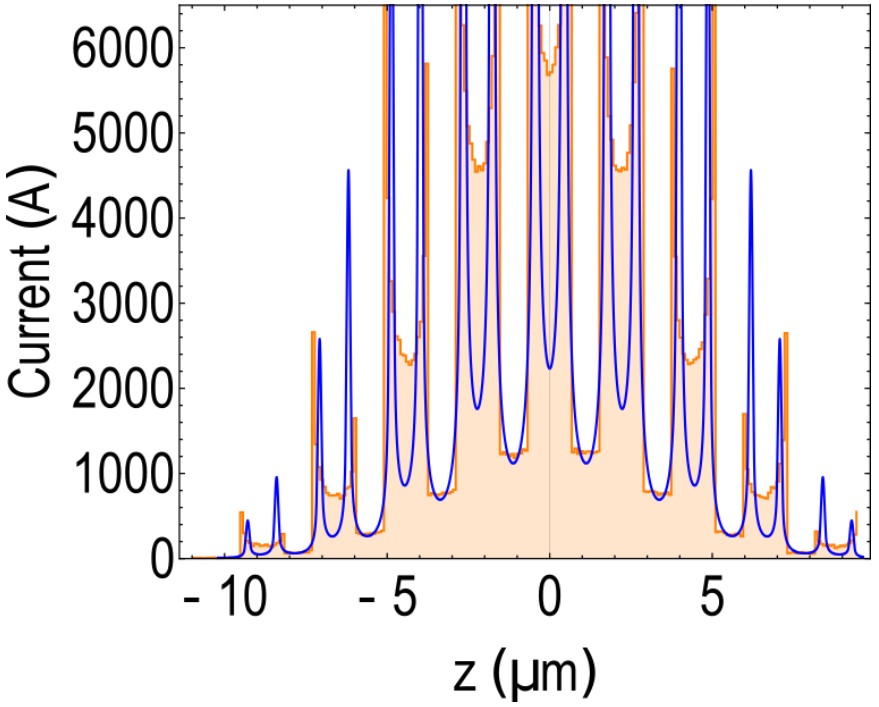

= analytical expression

= histogram, particle tracking data

Current profile analytical expressions – caustic region

Piecewise analytical functions (orange) can model the caustic current profiles.
(These are mono-energetic, longitudinal plane only.)

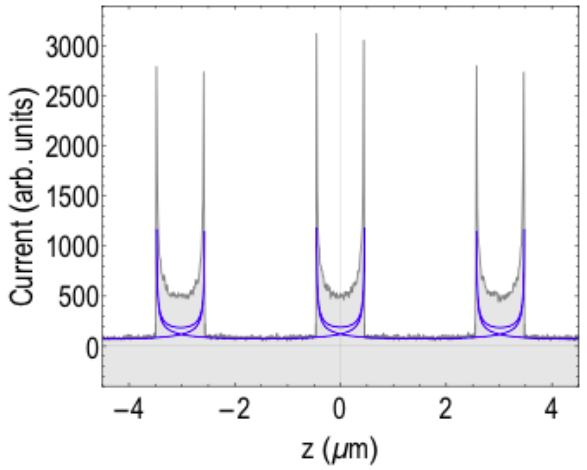

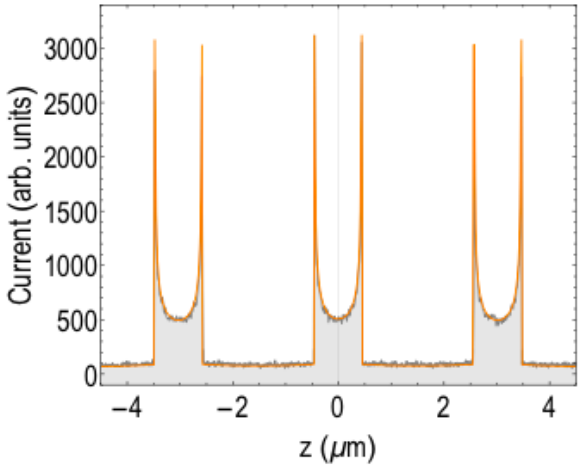

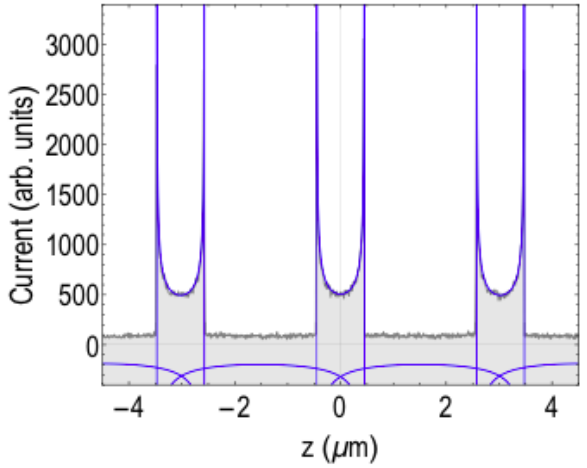

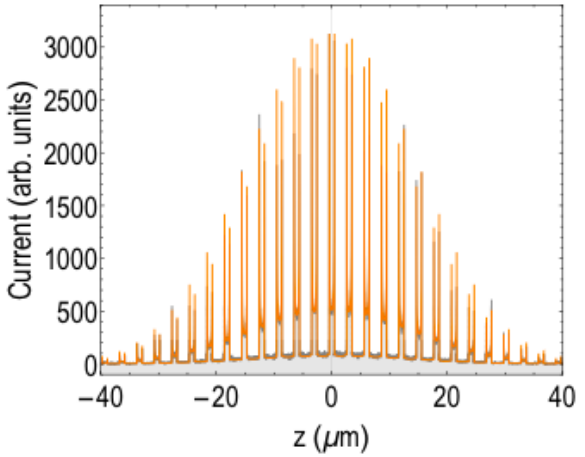

X-band linac example

R_{56} = -82.38 mm
T_{566} = 102.40 mm
U_{5666} = -5.23 m

R_{56} = -11.18 mm
T_{566} = 16.77 mm
U_{5666} = -11.10 mm

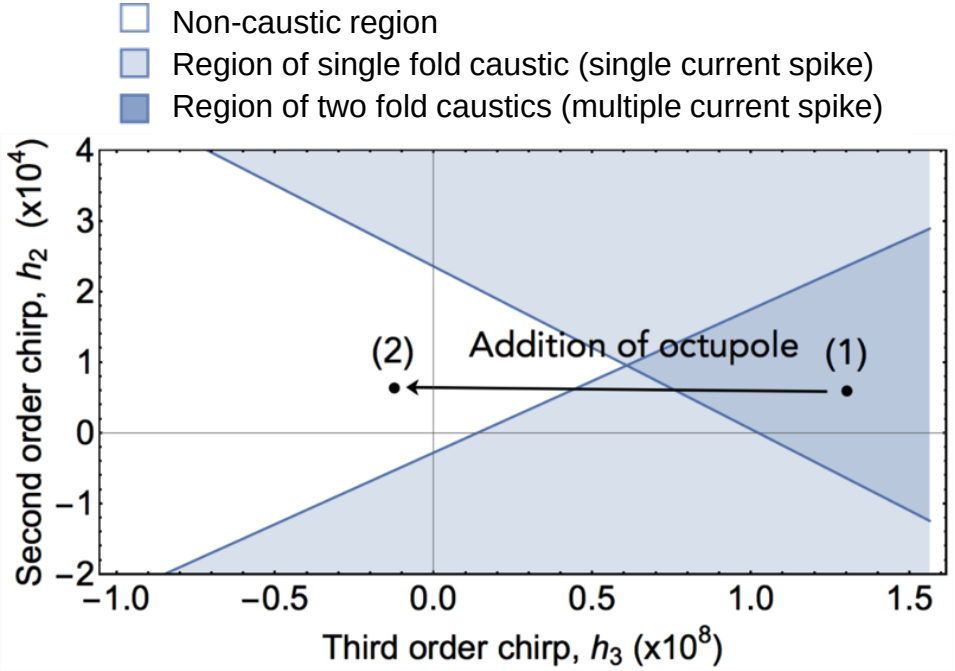

Without octupole:

With octupole:

Without CSR:

With CSR:

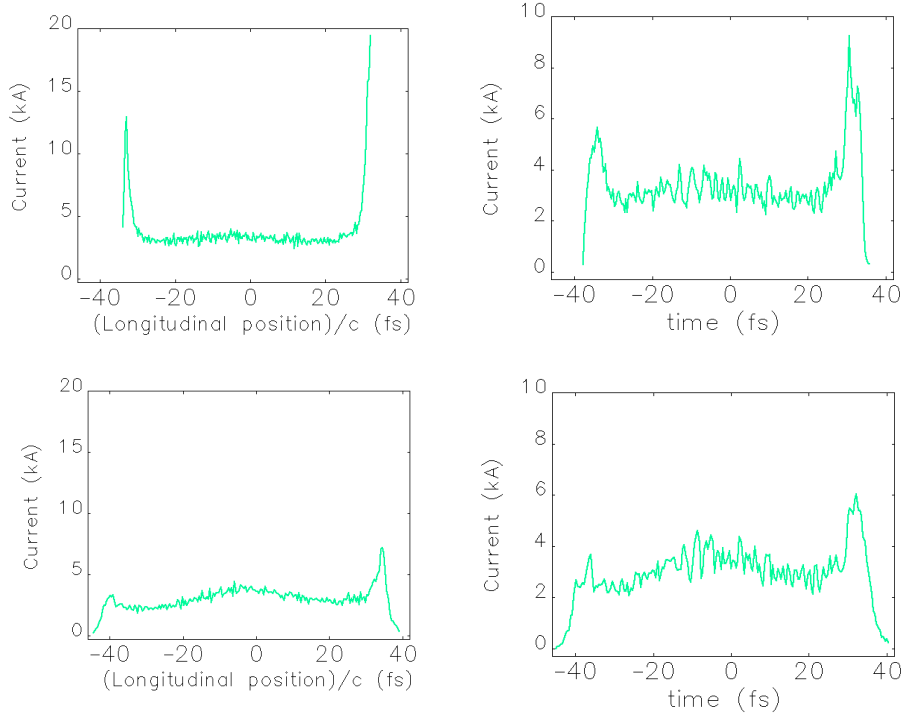

X-band linac example

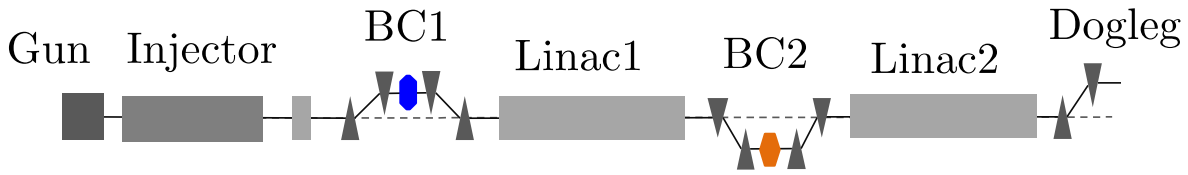

R_{56} = -82.38 mm
T_{566} = 102.40 mm
U_{5666} = -5.23 m

R_{56} = -11.18 mm
T_{566} = 32.05 mm
U_{5666} = -72.00 mm

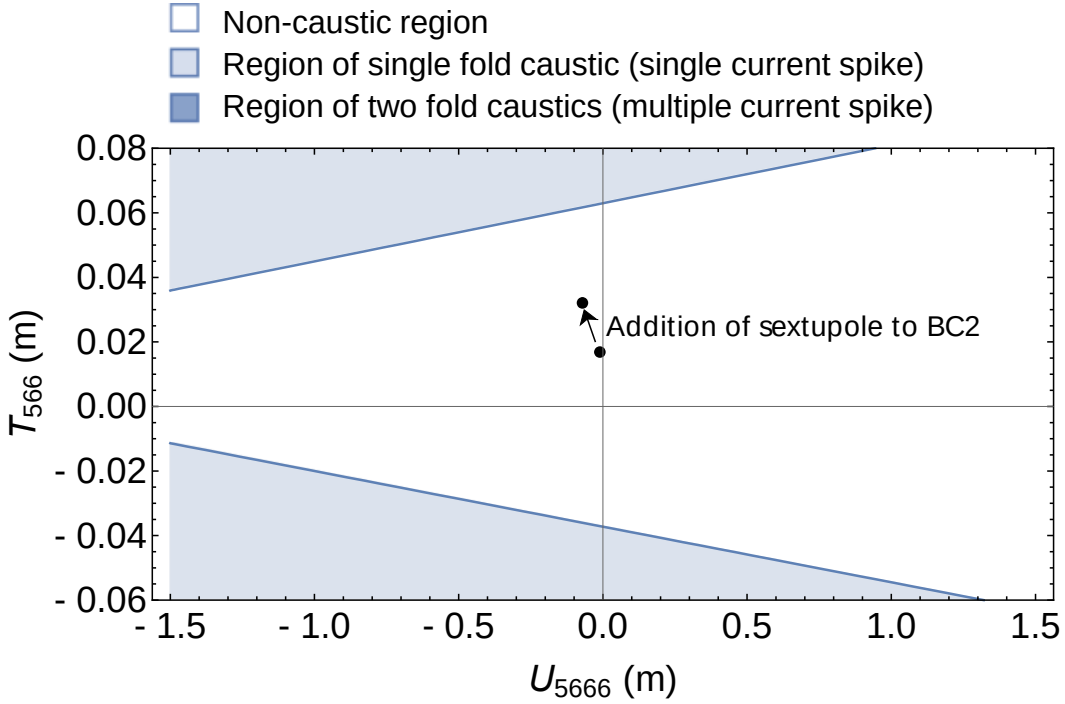

Without CSR: With CSR:

Without sextupole:

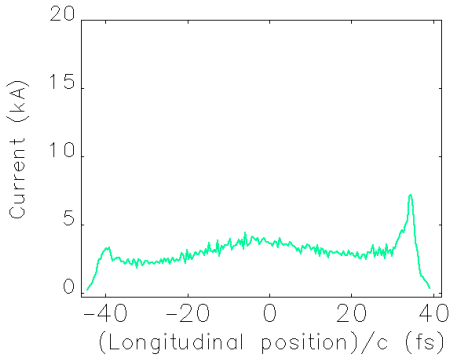

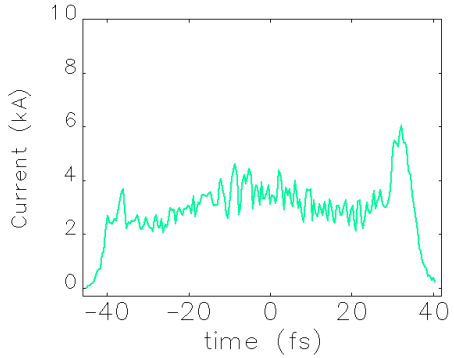

With sextupole:

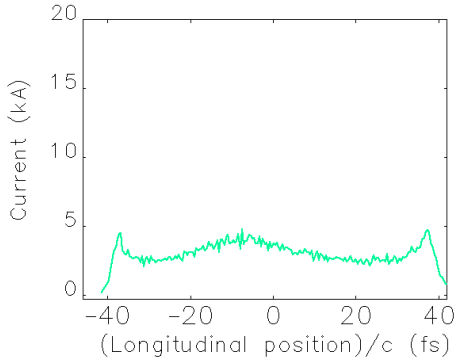

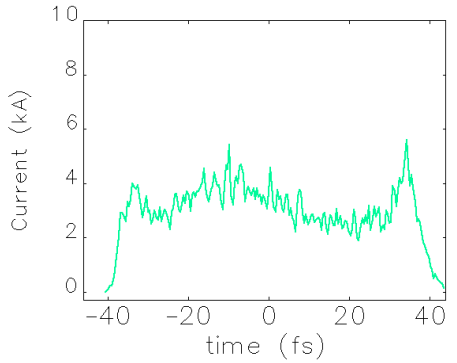

X-band linac example

X-band Linac

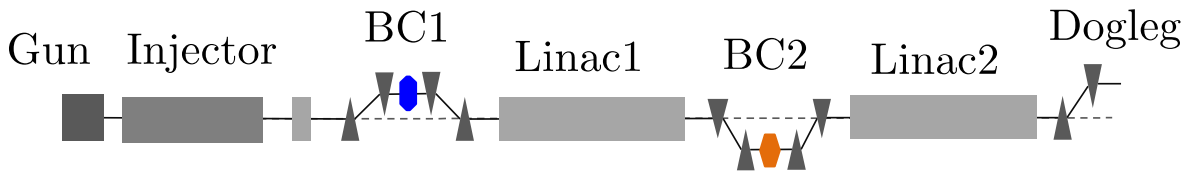

Bunch Compressor 1

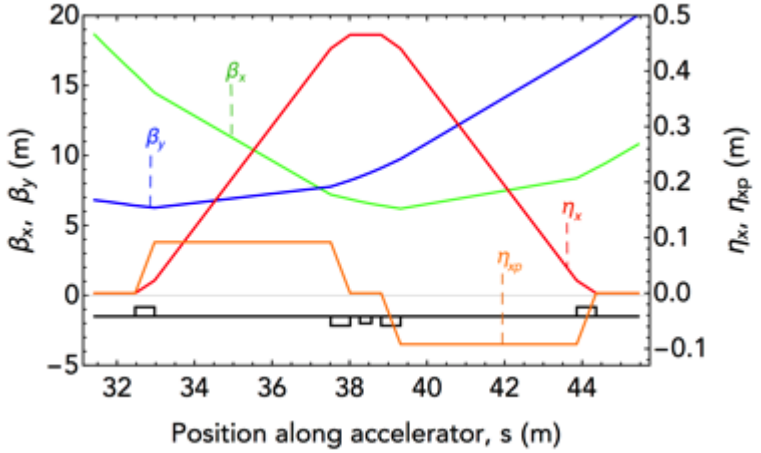

Bunch Compressor 2

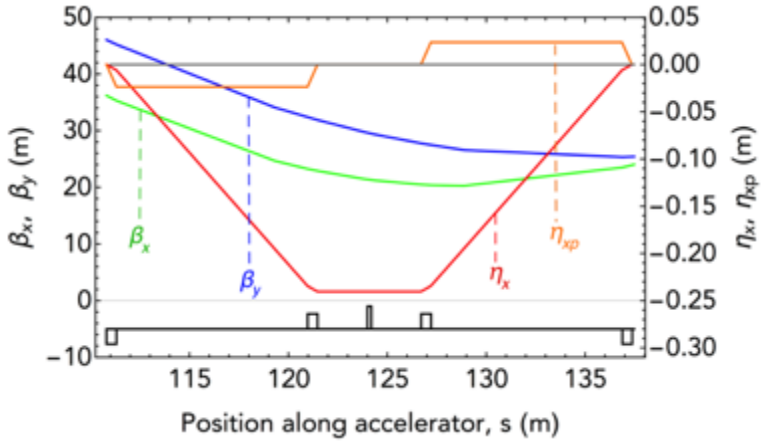

BC1:

R56 = -82.36 mm
T566 = 102.40 mm
U5666 = -5.23 m

Dipole bending angle, $\theta = 5.25°$
Octupole strength, K3 = 2061 m^{-4}

BC2:

R56 = -11.18 mm
T566 = 32.10 mm
U5666 = -72.19 mm

Dipole bending angle, $\theta = 1.35°$
Sextupole 1 strength, K2 = 11.03 m^{-2}

X-band linac example

X-band Linac

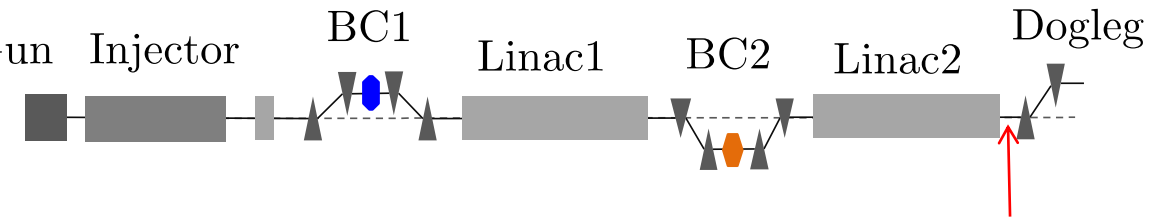

Without octupole & sextupole:

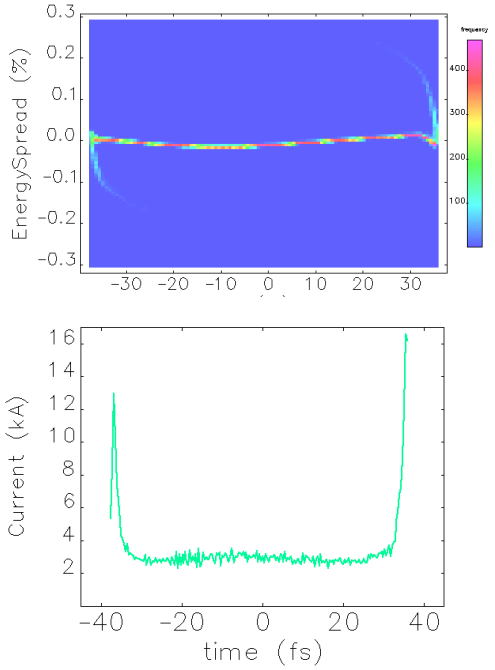

$\epsilon_{nx} = 1.394$ mm mrad

With octupole & sextupole:

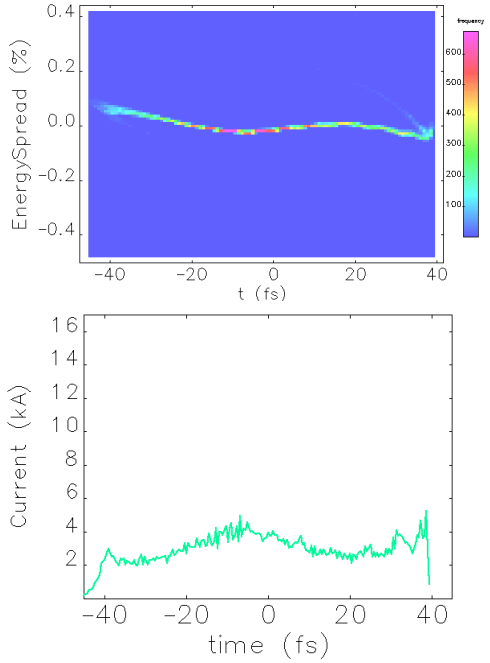

$\epsilon_{nx} = 0.842$ mm mrad

49% reduction in the CSR-induced emittance growth.

T. K. Charles *et al.* (2017) Phys. Rev. AB, 30, 030705

FFI : X-band linac

TABLE I: Beam properties at the end of the final linac section, for (a) Baseline layout, (b) Layout 1: which includes BC1 octupole magnet (Fig. 6a), (c) Layout 2 which includes BC2 sextupole magnet (Fig. 6b).

Parameter	Symbol	Units	Baseline	Layout 1	Layout 2
Bunch length	σ_z	μm	6.65	6.75	6.68
Horizontal bunch size	σ_x	μm	0.376	0.306	0.267
Vertical bunch size	σ_y	μm	0.161	0.162	0.163
Energy spread	$\sigma_{\Delta E/E}$	%	0.0371 (core)	0.0292	0.0281
Peak current	I_{peak}	kA	3.02 (core)	3.02	3.09
Total compression ratio	CR	-	121.38[a]	119.6	120.8
Bunch charge	Q	pC	250	250	250
Electron energy	E	GeV	6.16	6.16	6.16
Projected horizontal emittance	$\epsilon_{n,x}$	mm mrad	1.394	0.974	0.842
Mean horizontal slice emittance	$\epsilon_{s,n,x}$	mm mrad	0.386	0.392	0.377
Projected vertical emittance	$\epsilon_{n,y}$	mm mrad	0.274	0.273	0.274
Mean vertical slice emittance	$\epsilon_{s,n,y}$	mm mrad	0.255	0.249	0.246

[a] Note the bending angles of BC2 were reduced by less than 0.01% to bring the compression ratio down to be in-line with Layout 1 and Layout 2.

X-band linac, final bunch slice properties

X-band linac

Without octupole: •

With octupole: +

With octupole and sextupole: *